Role of the structural inheritance of the oceanic lithosphere in the magmato-tectonic evolution of Piton de la Fournaise volcano (La Réunion Island)

Laurent Michon, Francky Saint-Ange, Patrick Bachèlery, Nicolas Villeneuve, Thomas Staudacher

Role of the structural inheritance of the oceanic lithosphere in the magmato-tectonic evolution of Piton de la Fournaise volcano (La Réunion Island)

Laurent Michon,[1] Francky Saint-Ange,[1] Patrick Bachelery,[1] Nicolas Villeneuve,[2] and Thomas Staudacher[3]

Received 26 June 2006; revised 10 October 2006; accepted 3 November 2006; published 24 April 2007.

[1] La Réunion Island is located east of Madagascar, on the eastern rim of the tectonically inactive Mascarene Basin. This island is composed of three shield volcanoes of which only Piton de la Fournaise is currently active. Although the magmatic activity is restricted to Piton de la Fournaise, a scattered seismicity occurs on the whole 200 km wide volcanic edifice and in the underlying oceanic crust. We carried out a multiscale analysis to understand (1) the origin of the seismicity in the geodynamic context and (2) the role of the oceanic lithosphere in the deformation of Piton de la Fournaise and La Réunion Island. Analysis of the magmatic system suggests that the magma ascent is controlled by large N25–30 and N125–130 fracture zones located below the Enclos depression. We also show that the orientation difference between the eruptive fissures and the related dykes result from a rotation of the main principal stress σ_1 from vertical to downslope through the surface. Combining a Digital Elevation Model (DEM) analysis, field observations and the geophysical data reveals that the volcano is affected by large fault zones. The fault distribution indicates the predominance of a main N70–80 trend. Magnetic data show the same N80 orientation characterizing the remnant part of the Alizés volcano. Such parallel alignment suggests a control exerted by the underlying Alizés volcano on Piton de la Fournaise. Furthermore, the alignment between the crustal orientations and the structures determined on the island suggests a control of the crustal structures in La Réunion's volcano-tectonic activity. Contrary to several volcanic islands such as Hawaii and Tenerife, La Réunion volcanoes lie on an upbending crust. Then, we interpret the reactivation of the crustal faults as resulting from a crustal uplift related to the thermal erosion of the base of the lithosphere and/or to strong underplating. The upward deformation may prevent the spreading of the volcanoes, as no evidence of such a mechanism is observed in the bathymetry and the seismic data around the island.

Citation: Michon, L., F. Saint-Ange, P. Bachelery, N. Villeneuve, and T. Staudacher (2007), Role of the structural inheritance of the oceanic lithosphere in the magmato-tectonic evolution of Piton de la Fournaise volcano (La Réunion Island), *J. Geophys. Res.*, *112*, B04205, doi:10.1029/2006JB004598.

1. Introduction

[2] The building of an oceanic island is mainly induced by the development of a mantle plume at depth and its upwelling below the oceanic lithosphere [*Morgan*, 1971]. The volcanic activity resulting from the ascent of this mantle anomaly is frequently radially distributed around a volcanic center and concentrated in volcanic rift zones [e.g., *Walker*, 1999]. As documented for the Hawaiian volcanoes [*MacDonald and Abbott*, 1970] and the Society and Austral Islands [*Binard et al.*, 1991], the orientation of these rift zones is superimposed to main crustal orientations as transform zones and/or paleoridges. Active faulting is frequently associated with the volcanism. Fault analysis reveals that (1) normal faulting always prevails whatever the geodynamic context is and (2) faults and dyke swarms (i.e., rift zones) are parallel [*MacDonald and Abbott*, 1970; *Marinoni and Gudmundsson*, 2000]. As mentioned by *Binard et al.* [1991], such an alignment between tectonics and volcanism, and the rift zones and the crustal structures, respectively, suggests a control of the oceanic lithosphere on the deformation of shield volcanoes and on the location of the magmatism.

[3] La Réunion Island is located east of Madagascar and is related to the mantle plume that generated the Deccan

[1]Laboratoire des Sciences de la Terre de l'Université de la Réunion (LSTUR), Institut de Physique du Globe de Paris, CNRS, Saint Denis, France.
[2]CREGUR, Université de la Réunion, Saint Denis, France.
[3]Observatoire volcanologique du Piton de la Fournaise (OVPF), Institut de Physique du Globe de Paris, CNRS, La Plaine des Cafres, France.

0148-0227/07/2006JB004598$09.00

Traps at the Cretaceous-Tertiary boundary [*Courtillot et al.*, 1986; *O'Neill et al.*, 2003]. The island built up on an oceanic lithosphere characterized by N30–40 transform zones, predominant N120–130 trending magnetic anomalies [e.g., *Fretzdorff et al.*, 1998], and local N80 magnetic anomalies east of La Réunion (Figure 1a) [*Lénat et al.*, 2001]. The N120–130 orientation also corresponds to the overall elongation of the island, which results from the emplacement of three volcanoes along this axis (the Alizés, Piton des Neiges, and Piton de la Fournaise volcanoes; Figure 1b [*Lénat et al.*, 2001]). Contrary to Hawaiian volcanoes no active faults were identified at Piton des Neiges and Piton de la Fournaise, suggesting no or undetectable tectonic activity. However, the seismic monitoring carried out by the Piton de la Fournaise Volcano Observatory recorded numerous earthquakes originating in the crust below the island and its vicinity (Figure 2). More distant (~100 km) earthquakes, which cannot be precisely located with the current seismic network, occur below the submarine flanks of the edifice. Although the occurrence of earthquakes indicates an active tectonic regime, its origin and consequences in the development of the volcano are poorly understood.

[4] Using a multiscale and multidisciplinary analysis, we aim at studying the tectonic activity of La Réunion, integrating it at a lithospheric scale, and understanding the origin of the deformation, taking into account the regional geodynamics and the role of the mantle plume. We focus our work on four different scales: (1) the active magmatic system of PdF, (2) the overall edifice of PdF, (3) the island and the proximal submarine flanks, and (4) the oceanic crust in the island's vicinity. The magmatic system is studied through the analysis of the eruptive fissure and dyke distribution in the Enclos caldera. The tectonic structures of PdF are inferred from a combination of surface deformation derived from a 25 m resolution digital elevation model (DEM), available geophysical data such as seismic, self-potential, magnetic, and audiomagnetotelluric data, field observations, and aerial photographs. As the dense tropical vegetation makes most of the volcanic flanks inaccessible, the field observations are focused on the deep valleys which incise the volcano's western part. Structures of the southern and northern flanks are studied with the DEM and the available geophysical data. At the island scale, a 100 m resolution DEM, gravimetric and magnetic data and sonar images are used to determine the first order subaerial and submarine structures. Finally, the magnetic crustal structures and the oceanic floor topography are integrated in our study to extend the analysis from a kilometer scale to a several hundred kilometers scale.

2. Geological Setting

[5] La Réunion Island is the subaerial part of a 7 km high oceanic shield volcano with a diameter of 220–240 km. Considering the historical magma production rate and the oldest dated subaerial basalts (~2 Ma [*MacDougall*, 1971]), an age of around 5 Ma was estimated for the beginning of the edifice growth [*Gillot et al.*, 1994]. The initial evolution was characterized by the development of two adjacent volcanoes (Piton des Neiges and Alizés volcanoes), which encountered recurrent flank destabilizations [*Lénat et al.*, 2001; *Bachèlery et al.*, 2003; *Oehler et al.*, 2004]. Around 530 ka ago, Piton de la Fournaise appeared west of the Alizés volcano which stopped its activity. Between 530 ka and 12 ka (date of the last eruption of Piton des Neiges (PdN) [*Deniel et al.*, 1992]) PdN and PdF showed contemporaneous activity. Finally, since 12 ka, eruptions are restricted to PdF.

[6] This multiphase evolution made the structure of the overall edifice of La Réunion very complex. The Alizés volcano is now completely dismantled and the only evidence of its past existence is (1) a large intrusion complex identified by drilling below the Grand Brûlé (Figure 3) [*Rançon et al.*, 1989], (2) the remnant old submarine relieves [*Labazuy*, 1996], and (3) the pre-Brunhes reverse magnetic anomalies which characterize magmatic formations older than those of Piton de la Fournaise [*Lénat et al.*, 2001].

[7] Piton des Neiges results from a more than 2 m.y. long activity during which construction and dismantling phases alternated. The oldest parts correspond to La Montagne, the Dimitile, and Takamaka massifs (Figure 3). The other volcano flanks consists on piles of differenciated lava flows which date from the volcano's late activity, some 350 ka ago. Large explosive eruptions occurred during this period [*Fretzdorff et al.*, 2000]. The volcano's central part exhibits three major depressions: the cirques of Cilaos, Mafate, and Salazie, which originate from an intense erosion controlled by structural limits such as large landslides [*Oehler et al.*, 2004]. In the depressions, most of the outcropping formations are intensively weathered rocks and debris avalanche deposits, intruded by a large number of dykes [*Chevallier*, 1979; *Maillot*, 1999].

[8] Piton de la Fournaise is the active volcano of La Réunion Island. Geochronological and geological data allow defining two main phases of construction, separated by a main collapse event: the "ancient Fournaise" (530–150 ka) and the "recent Fournaise" (150 ka to present day) [*Gillot and Nativel*, 1989; *Bachèlery and Mairine*, 1990; *Gillot et al.*, 1990]. This large landslide led to an eastward shift of the volcano center from the present-day location of the Plaine des Sables to the current position of the active volcano. During the last 0.15 Ma, the "recent Fournaise" was affected by at least two caldera collapses whose exact origin is still under debate [*Bachèlery*, 1981; *Duffield et al.*, 1982; *Gillot et al.*, 1994; *Labazuy*, 1996; *Merle and Lénat*, 2003]. The resulting structures are the Plaine des Sables and the large U-shaped structure composed of the Enclos depression and the Grand Brûlé (Figure 3). Since the formation of the Enclos depression 4.5 ky ago, the volcanic activity is mainly restricted to the caldera. Only few eruptions occurred along the NE and SE rift zones, in the Plaine des Sables and in the Rivière des Remparts [*Bachèlery*, 1981].

[9] Intense erosion incised the edifice leading to the formation of deep valleys (Rivière des Remparts, Rivière Langevin, Rivière Basse Vallée, and Rivière de l'Est (Figure 3). An additional erosional structure was discovered on the eastern flank of PdF. Geophysical data (audiomagnetotelluric and time domain electromagnetic) and cores with fluvial sediments from a drill hole in the northern part

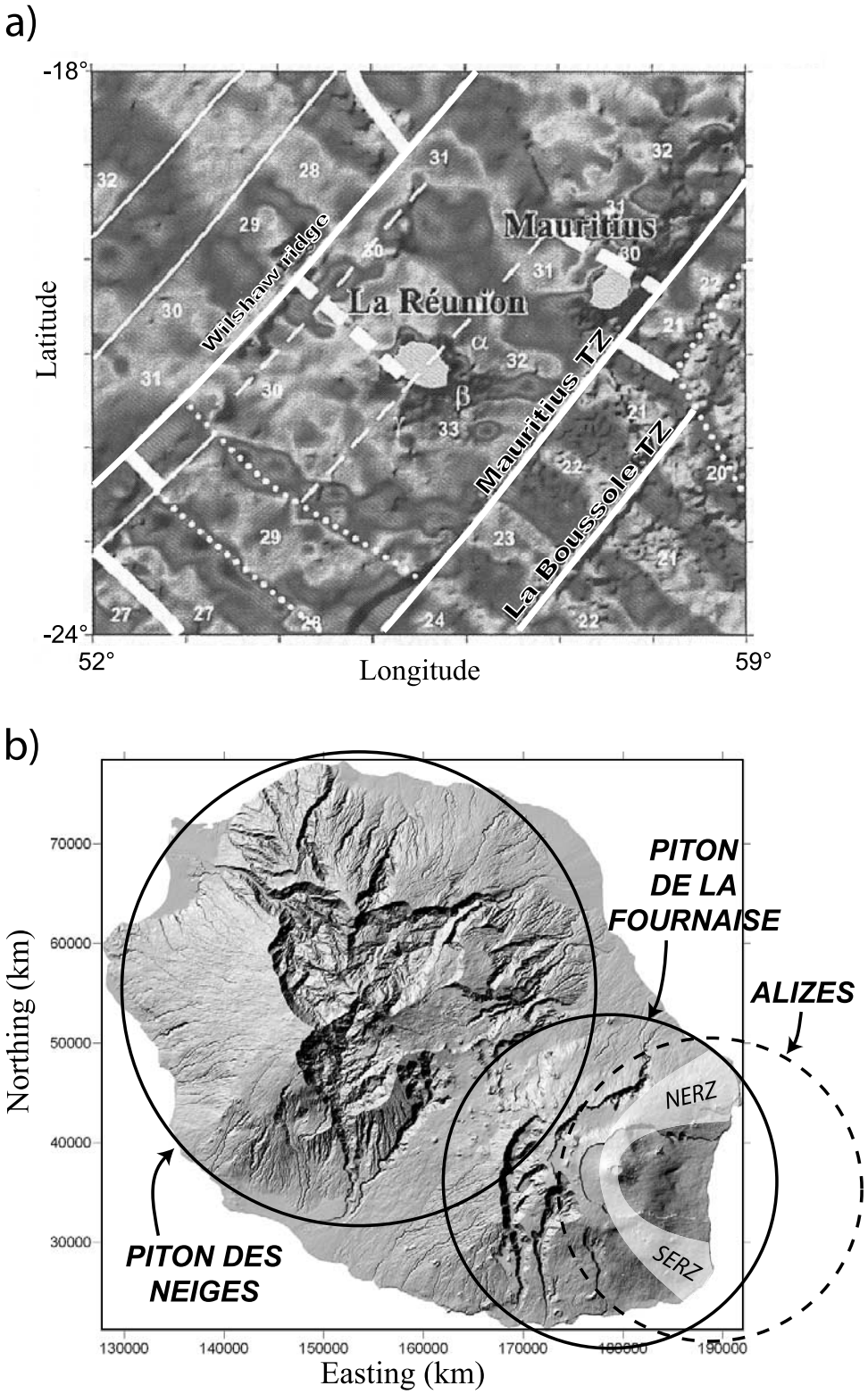

Figure 1. a) Map of the crustal magnetic anomalies in the vicinity of La Réunion and Mauritius Islands. Transform zones trend N30–40 while the magnetic anomalies present a N120–130 orientation. After *Lénat et al.* [2001]. (b) Location of the three basaltic volcanoes that constructed La Réunion Island. SERZ: Southeast rift zone; NERZ: Northeast rift zone.

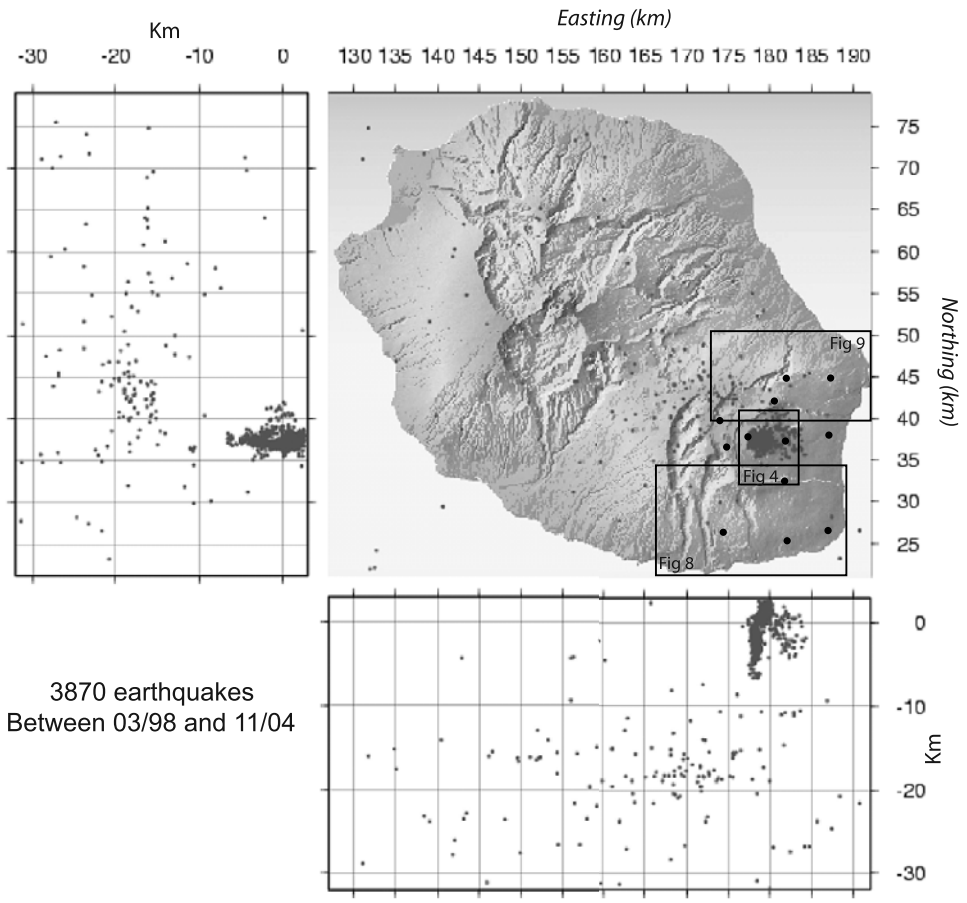

Figure 2. Map of the post-1997 seismicity occurring on La Réunion Island. Location of Figures 4, 8, and 9 is indicated by rectangles. Black dots represent the seismic stations of the Piton de la Fournaise Volcano Observatory.

of the Grand Brûlé reveal the presence of the Osmondes paleoriver [*Courteaud*, 1996].

3. Multiscale Structures of the Piton de la Fournaise

3.1. Structure of the Magmatic System

[10] During the eruptions of PdF, magma ascent mainly leads to the formation of eruptive fissures in the Enclos and on the flanks of the central cone. Most of the eruptions induce the development of en échelon eruptive fissures, which are commonly interpreted as the result of lateral shear during the dyke intrusion [e.g., *Bachèlery et al.*, 1983; *Lénat et al.*, 1989; *Zlotnicki et al.*, 1990]. According to these studies the northern and southern rift zones are characterized by left lateral and right lateral deformation, respectively, which would contribute to the eastward destabilization of the volcano flank. Although this general view is well established, we believe that it raises several questions. Are the eruptive fissures adequate to determine the rift zone orientation? Is the en échelon geometry an evidence of lateral shear along the rift zones?

3.1.1. Eruptive Fissures and Feeder-Dyke Orientation

[11] The visible pre-2003 eruptive fissures are predominantly oriented along three main directions (N10–20, N70–80, and N170), which are in agreement with the three trends determined by *Bachèlery* [1981] (Figure 4). The N10–20 and N170 trends are interpreted as the upper part of the NE and SE rift zones, named the N10 and N170 rift zones, respectively [*Bachèlery*, 1981], and were inferred from the eruptive fissure distribution [*Bachèlery*, 1981]. A detailed inspection of the recent en échelon eruptive fissures clearly shows that both orientations can develop during a single event (e.g., the March 1998 eruption, August 2003) and that N170 eruptive fissures also form in the northern flank, which is commonly described as the "site of the N10 rift zone" (Figure 5). Figure 5 reveals en échelon fissures which are parallel or subparallel to the slope. This distribution of the recent fissures is common to most of the visible pre-2003 eruptive fissures (Figure 4). Only a few are linear and oblique to the slope (e.g., the August 2004 eruption). Their constant orientation and location east of the Dolomieu crater could indicate a control of local subsurface structures in the fissure development.

[12] As for Stromboli [*Tibaldi*, 2003] and Etna [*MacGuire and Pullen*, 1989], it has been recently shown for the March 1998 [*Battaglia and Bachèlery*, 2003], February 2000, June 2000, and August 2003 eruptions [*Peltier et al.*, 2005] that the orientation of the en échelon eruptive fissures do not represent the orientation of the magmatic dyke at depth. Moreover, numerical models show that the en échelon pattern results from the intrusion of linear dykes at

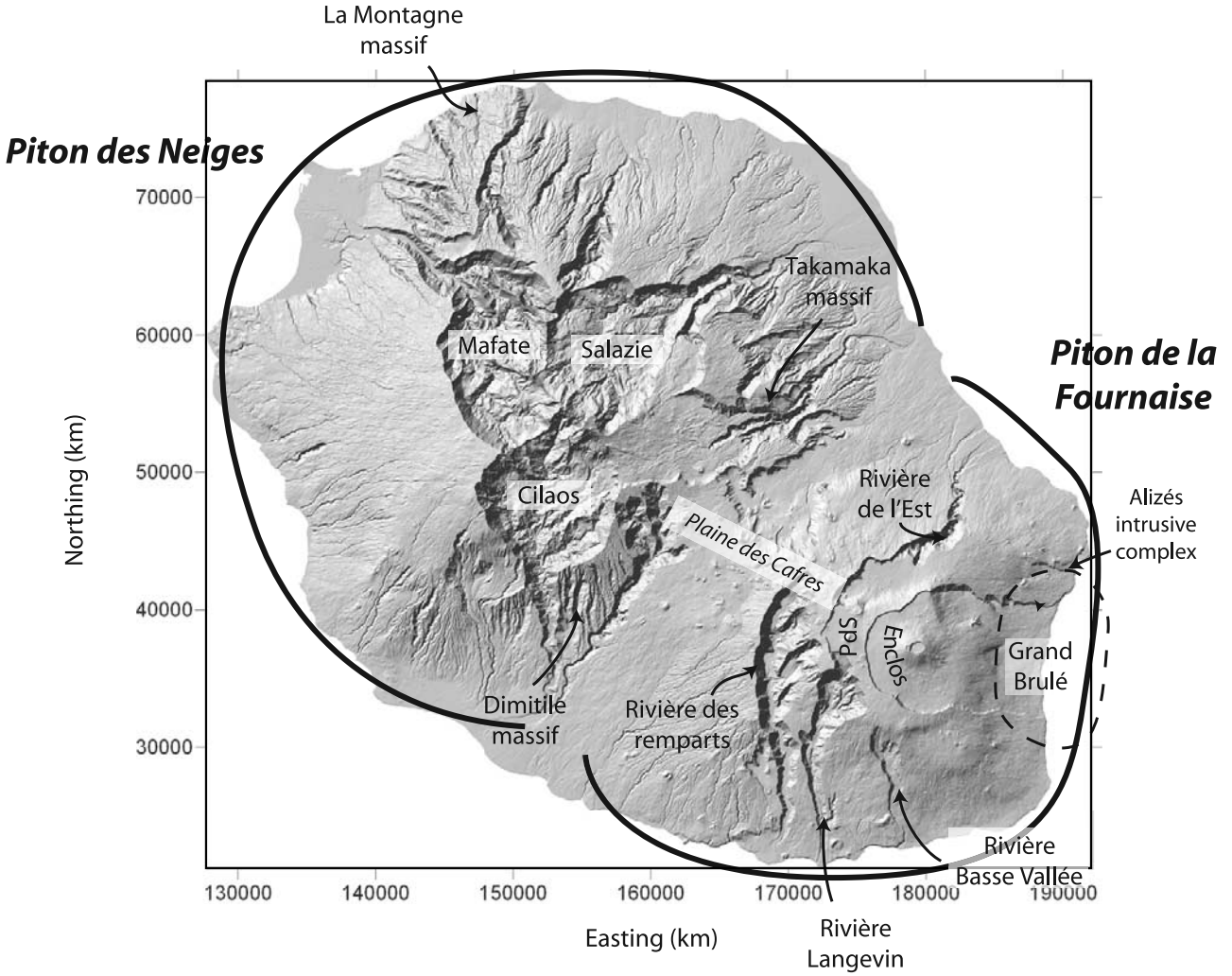

Figure 3. Overview of the main geological structures of La Réunion Island discussed in the text. PdS: Plaine des Sables.

depth [*Cayol and Cornet*, 1998; *Battaglia and Bachèlery*, 2003; *Fukushima et al.*, 2005; *Peltier et al.*, 2005]. Considering these results, we compared the orientation of 17 dykes for the 1998–2004 period with the distribution of the 63 eruptive fissures formed during the same time span (Figure 6a). It appears that the fissure and dyke orientations differ from each other.

3.1.2. Dyke, Fissure, and Stress Field

[13] As dykes and eruptive fissures are strongly sensitive to the stress distribution (σ_3 and σ_1, the least and main principal stress component, respectively), the difference in the orientation between dykes and fissures suggests distinct stress field orientations at depth and near the surface. In a homogeneous volcanic cone, σ_3 is perpendicular to the slope and σ_1 varies from a vertical orientation at depth to a downslope one in subsurface [*van Wyk de Vries and Matela*, 1998]. Note that the magnitude of the downslope σ_1 increases through the surface [*Borgia*, 1994]. In such an ideal cone, eruptive fissures and dykes, which correspond to tension cracks are radially distributed [*Pollard*, 1987]. However, in nature additional effects such as magma overpressure, contrasted rheological layering, volcano instabilities, faulting activity and structural inheritance lead to a strongly anisotropic stress field, which may influence the dyke intrusion along preferential orientations [*Chadwick and Dieterich*, 1995; *Tibaldi*, 1996, 2003; *Walker*, 1999; *Marinoni and Gudmundsson*, 2000; *Walter and Troll*, 2003; *Gudmundsson*, 2006].

[14] At PdF the radial to subradial distribution of the eruptive fissures and the deformation field observed through interferometry and only showing deformation perpendicular to the dyke [*Sigmundsson et al.*, 1999; *Froger et al.*, 2004; *Fukushima et al.*, 2005] suggest that the fissure orientation is controlled by downslope σ_1 rather than by the lateral shear during the dyke intrusion. According to the numerical models simulating the coeruptive deformation observed in interferometry [*Fukushima et al.*, 2005], the transition depth at which the dykes transform into eruptive fissures, that is the depth at which σ_1 rotates from vertical to downslope, evolves from ~200 m below the top of the cone to ~100 m below the base of the cone. Such variation agrees with the distribution of the downslope σ_1 which affects a greater vertical section close to the top of a cone than at its base [*van Wyk de Vries and Matela*, 1998].

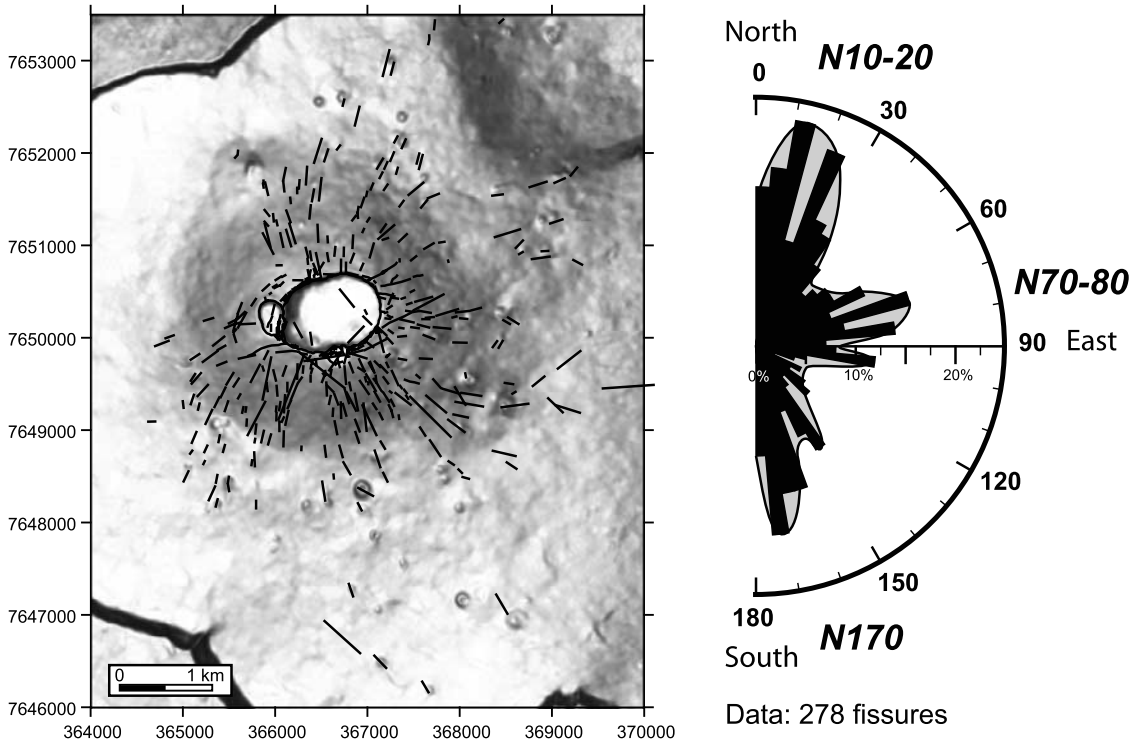

Figure 4. Distribution of the pre-2003 eruptive fissures visible in the summit part of Piton de la Fournaise. Eruptive fissures trend in three main directions: N10–20, N70–80, and N170. Coordinates in meters (WGS 84).

3.1.3. Rift Zone Orientation

[15] In contrast to the fissure distribution, the dyke distribution for post-1997 eruptions is far from radial. More than 70% of the eruptions are concentrated in two zones (i.e., the N25–30 and N125–130 intrusion trends) suggesting that the dyke emplacement is controlled at depth (Figure 6a). These two trends strikingly coincide with the two positive self-potential (SP) anomalies, determined in 1992–1993 by *Michel and Zlotnicki* [1998], during the 1993–1997 gap of activity, and 5 years before the beginning of the post-1997 eruptive cycle. Positive SP anomalies up to 1000 mV indicate upward fluid flow which originates from permanent preferential fluid migration along a fracture zone or from a recent dyke intrusion. Figure 6b shows that some small-scale anomalies (few hundred of meters) are correlated with the eruptive fissures of 1987 and 1988 in the northern part of the N25–30 intrusion trend. However, it also reveals that these anomalies are of small-scale compared to the 1–2 km wide N30 and N125 SP anomalies. This suggests that the large N30 and N125 SP anomalies cannot be explained by the recent dyke-induced fluid circulation only. Therefore following *Michel and Zlotnicki* [1998], we believe that the large SP anomalies are caused by the upward fluid migration along fracture zones [*Michel and Zlotnicki*, 1998]. Moreover, (1) the superposition of the N25–30 and N125–130 intrusion trends, inferred from the post-1997 dyke distribution and the N30 and N125 SP anomalies, and (2) the recurrence of most of the eruptions (during the 1981–1992 period and since 1998) along the preferential magmatic paths, suggest that the magma ascent in the Enclos is controlled by a large, 10 km-long, N25–30 trending fracture zone and a secondary fracture trending N125–130.

[16] *Lénat and Bachèlery* [1990] and *Fukushima* [2005] proposed that the overpressure due to each dyke intrusion along one rift zone temporally prevents another intrusion along the same rift zone. This would subsequently explain the alternation of the eruptions along the northern and southern segments of the N25–30 rift zone and the N125–130 rift zone. However, the succession of three eruptions between October 2000 and June 2001 along the same N125–130 rift zone partly contradicts this model. Indeed, although each dyke increased the overpressure (i.e., the stress perpendicular to the intrusion), the next magma intrusion followed the N125–130 fracture zone. Such a recurrence along the N125–130 rift zone reveals the control of the fracture zone in the magma migration. At PdF, the guiding role of the N25–30 and N125–130 fracture zones is explained by the quasi-isostatic stress state [*Cayol and Cornet*, 1998] and a likely weaker Young's modulus within the fracture zone than in the surrounding parts [*Gudmundsson*, 2002; *Peltier et al.*, 2005].

[17] In summary, we cannot confirm the existence of the N10 and N170 rift zones as previously described. We agree that one main magmatic path controls the magma intrusion north of the cone. However, a unique N170 rift zone disagrees with the present data for the southern part. The fan shape geometry of the SE and NE rift zones outside the Enclos (Figure 1b) suggests that magmatic intrusions are not as controlled as in the Enclos. This indicates that once the magma reaches the limit of the Enclos caldera, its

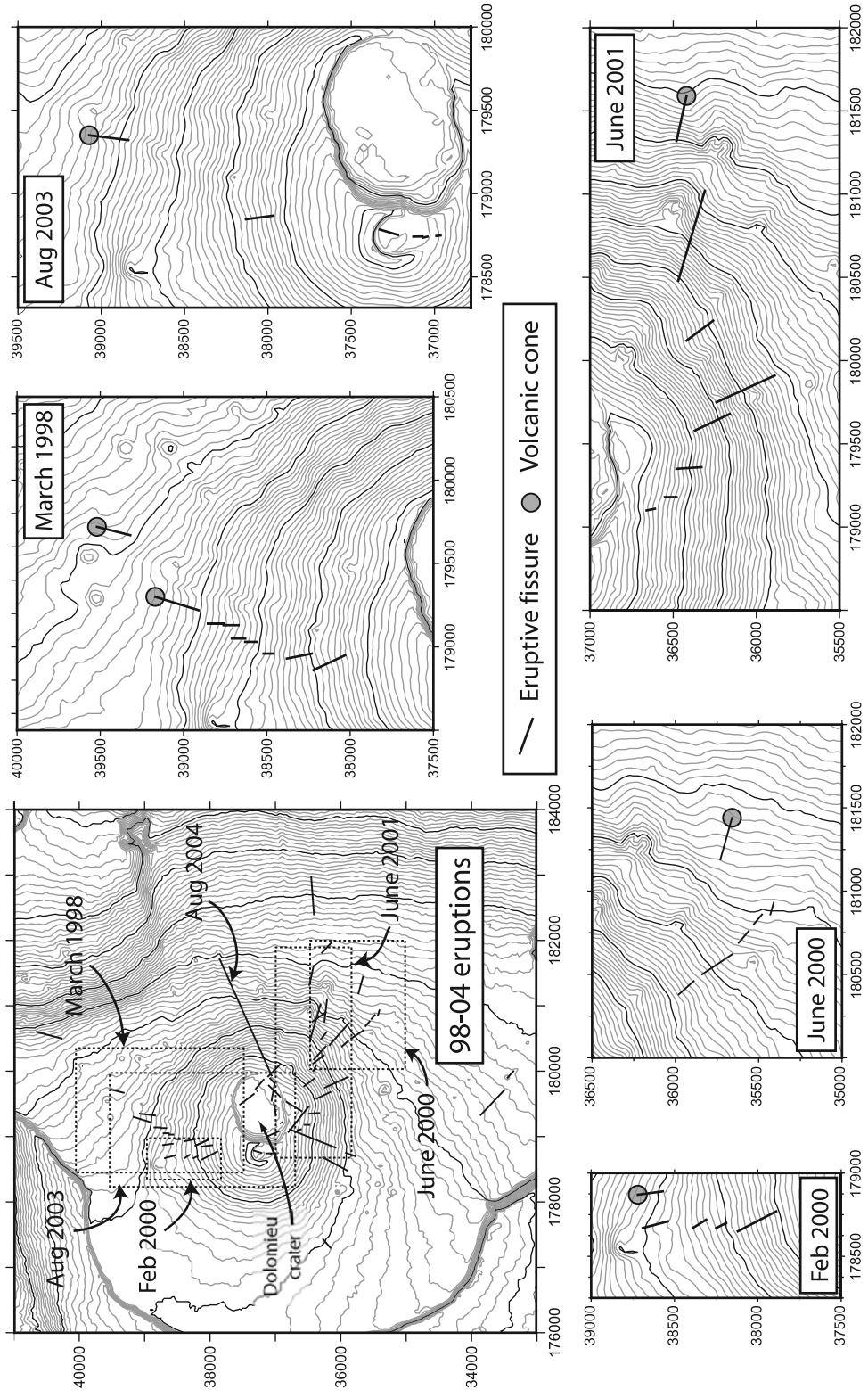

Figure 5. Distribution of the 1998–2004 eruptive fissures. En échelon patterns develop for most of the eruption: March 1998, February 2000, June 2000, June 2001, August 2003. Coordinates in meters (Gauss Laborde–Réunion).

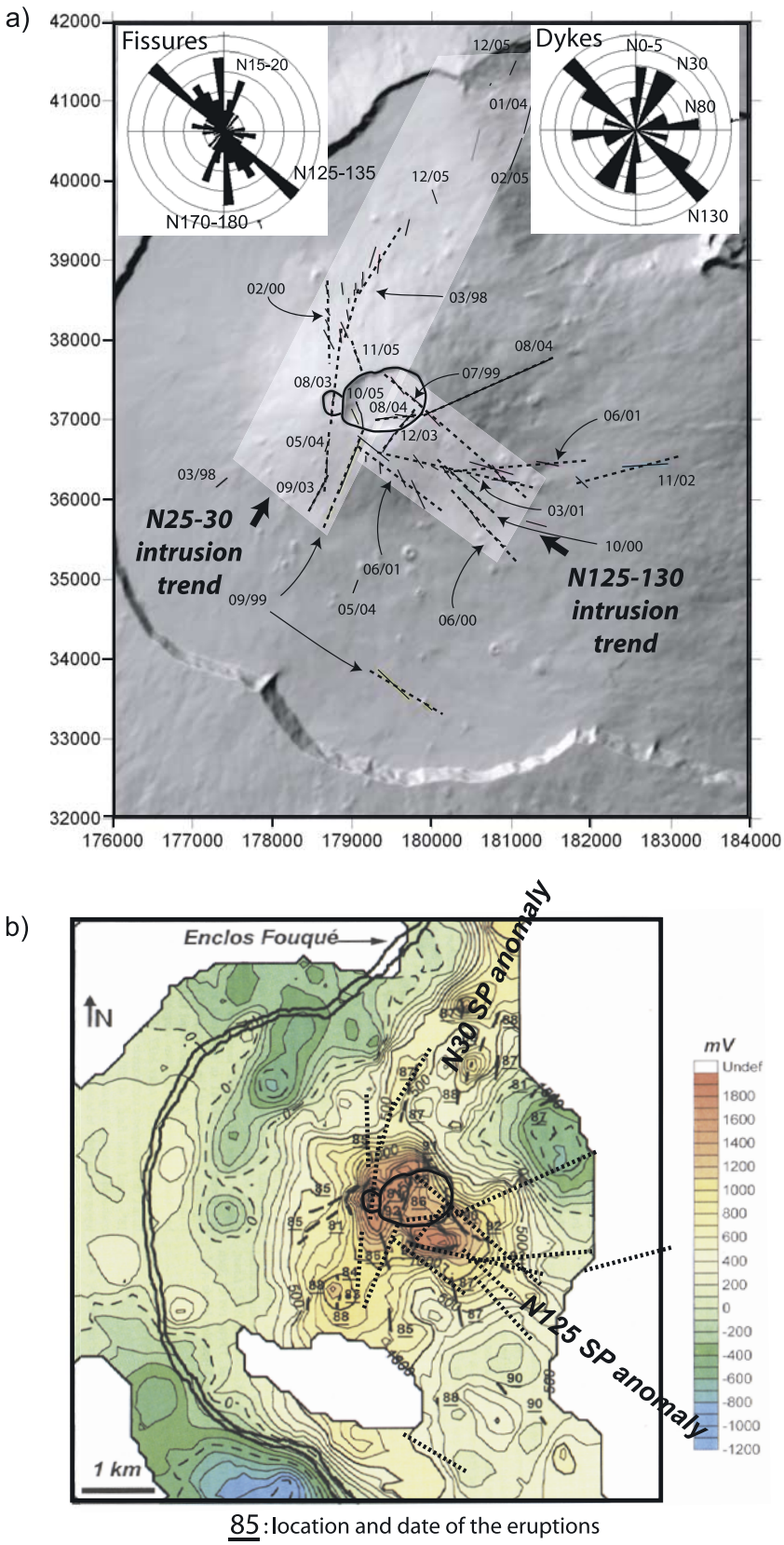

Figure 6. (a) Post-1997 eruptive fissures and the related dykes (dotted lines). The dyke distribution highlights two main N25–30 and N125–130 intrusion trends. Coordinates in meters (Gauss Laborde–Réunion). (b) Distribution of the post-1997 dykes (dotted lines) with respect to the Self-Potential anomalies measured by *Michel and Zlotnicki* [1998].

propagation is controlled by the stress field of the shallow edifice rather than by deep, narrow fracture zones.

3.2. Edifice Structures

3.2.1. Field Observations

[18] As the flanks of PdF are covered by either a dense vegetation or recent lava flows, we carried out a structural analysis in the deep valleys where geological units outcrop at the base of the scarps. We focused our analysis in the Rivière des Remparts and Rivière Langevin where the formations of the "ancient" and current Fournaise outcrop in 1000 m high scarps. Although dense vegetation covers most of the scarps, combination of structural and aerial photograph analysis allows determination of several main faults (Figure 7a). A large N05 trending, 15 km long fault zone is observed in the Rivière des Remparts inducing at different locations intense brecciation of the lava flows. In the southern half of the Rivière des Remparts, the fault zone controls the valley orientation and dyke emplacement (site 1 in Figure 7b). Further to the north (i.e., in the Mahavel and Bras Caron valleys), the fault zone, which is inaccessible but visible in aerial photographs is composed of several segments that induced a left-lateral offset of another subperpendicular fault (i.e., the N95 normal fault visible in the Rivière Langevin; Figure 7a). At site 1, geological formations do not show any vertical offset, suggesting a strike-slip motion along the fault plane. Although this outcrop is of small size the strike-slip motion is in agreement with the observation obtained further north by an aerial photograph.

[19] The second main fault presents a N40 orientation and is continued up in the scarp. The fault plane is characterized by constant subhorizontal slickenside, which indicates a right lateral movement with a slightly normal component (site 2 in Figure 7b). The fault plane outcrop is punctual and its lateral continuity cannot be determined directly. Nevertheless, it is interesting to note that the fault is in the western continuity of the Mahavel valley. Recent analogue models show that incisions of such deep valleys in volcanic settings result in structurally controlled erosion [*Fèvre et al.*, 2004]. This indicates that erosion, which led to the valley formation, was favored by the presence of the N40 trending fault. A third main fault is located in both the Rivière des Remparts and Rivière Langevin. In the Rivière Langevin this N95 trending fault affects both the tabular lava flows of the "ancient" Fournaise and the inclined lava flows of the recent Fournaise (60–70 ky) (site 3 in Figure 7b). The fault activity which is younger than 60 ky induced a vertical offset of around 100 m. This N95 fault being slightly disturbed by the N05 fault, a maximum age of 60 ky can be attributed to the last activity of the N05 trending fault.

[20] Thus field observations demonstrate that large faults developed during the Piton de la Fournaise evolution. However, it remains to be shown whether the faults are related to the PdF's own evolution or to the regional stress field.

3.2.2. DEM Analysis

[21] The flanks of Piton de la Fournaise are covered by tropical vegetation which prevents any field observation. To fill this gap, we combine the analysis of a 25 m DEM with the available geophysical data to extend the structural analysis to the whole flanks of PdF. In the southern flank, an audiomagnetotelluric (AMT) survey revealed the occurrence of two N65 and N145–150 trending preferential orientations of the subsurface basement, which are interpreted as large structural discontinuities (Figure 8) [*Courteaud et al.*, 1996]. The slope map shows the presence of numerous lineaments, which can have different origins. To prevent any integration of human-made structures and boundaries of geological formations such as lava flows and the river patterns, we compared the lineaments with geological and topographic maps. We consider only kilometer-scale and well-developed lineaments. Once rivers and the margins of the geological formations are excluded, the DEM shows two predominant lineament trends: a large N80 lineament on both sides of the Basse Vallée River and N155 lineaments parallel to the Basse Vallée River (Figure 8). The lack of geophysical data at the lineament location does not allow the study of their origin. Moreover, the extremely dense vegetation makes direct observation of the structures in the scarp of Basse Vallée absolutely impossible. It has been proposed that the basement structures in the lower part of the southern flank most likely correspond to faults [*Courteaud et al.*, 1996]. The alignment of these faults with the lineament trends inferred from the DEM analysis (N65–80 and N145–155) suggests a tectonic origin of the lineaments. Further studies are required to constrain better the exact origin of these structures.

[22] In the northern flank of PdF, two different slope domains can be determined from the slope orientation map (Figure 9a). Domains 1 and 2 are characterized by regular eastward and north-north-eastward slopes, respectively. In a homogeneous setting, rivers flow downslope. One striking exception is the Ravine Bellevue in domain 2, which flows in a N70–75 orientation that is strongly oblique to the slope. The development of straight and abnormally oriented rivers is usually due to a structural control [e.g., *Twidale*, 2004]. The pattern and orientation of Ravine Bellevue suggest that its formation was controlled by a N70–75 trending structure. This interpretation is supported by two sets of geophysical data. First, two-dimensional magnetic profiles carried out in the lower part of the flank reveals strong reverse magnetic anomalies below the Piton Balmann and 500 m south of the Piton Bellevue (Figure 9b) [*Michel and Zlotnicki*, 1998]. Reverse magnetized structures predate the Bruhnes period (normal magnetization since 0.78 My) and are consequently older than the formation of PdF. It is likely that these structures correspond to a remnant part of the Alizés volcano [*Michel and Zlotnicki*, 1998], which shows in this area a N75 orientation. The second set of data is located in the upper part of the Rivière de l'Est where 19 seismic events were recorded from 1985 to the end of 1988 (Figure 9b) [*Nercessian et al.*, 1996]. These events, which occurred outside the present-day magmatic zone between 6 km b.s.l. and the surface, are disconnected from any recognized faults. Nevertheless, the earthquake distribution along a N70–75 main axis suggests the occurrence of a deep and active N70–75 fault. Hence the combination of the geophysical data and DEM analysis suggests that the northern flank of PdF is affected by a N70–75 fault zone, the

development of which was likely controlled by structures that also influenced the evolution of the Alizés volcano.

[23] The DEM analysis allowed us to extend the structural analysis to the PdF southern and northern flanks. Our work suggests the predominance of large N65–80 trending fault zones outside the Enclos-Grand Brûlé structure and secondary N145–155 faults. It is worth noting that the fault orientation differs from the field observations. This differ-

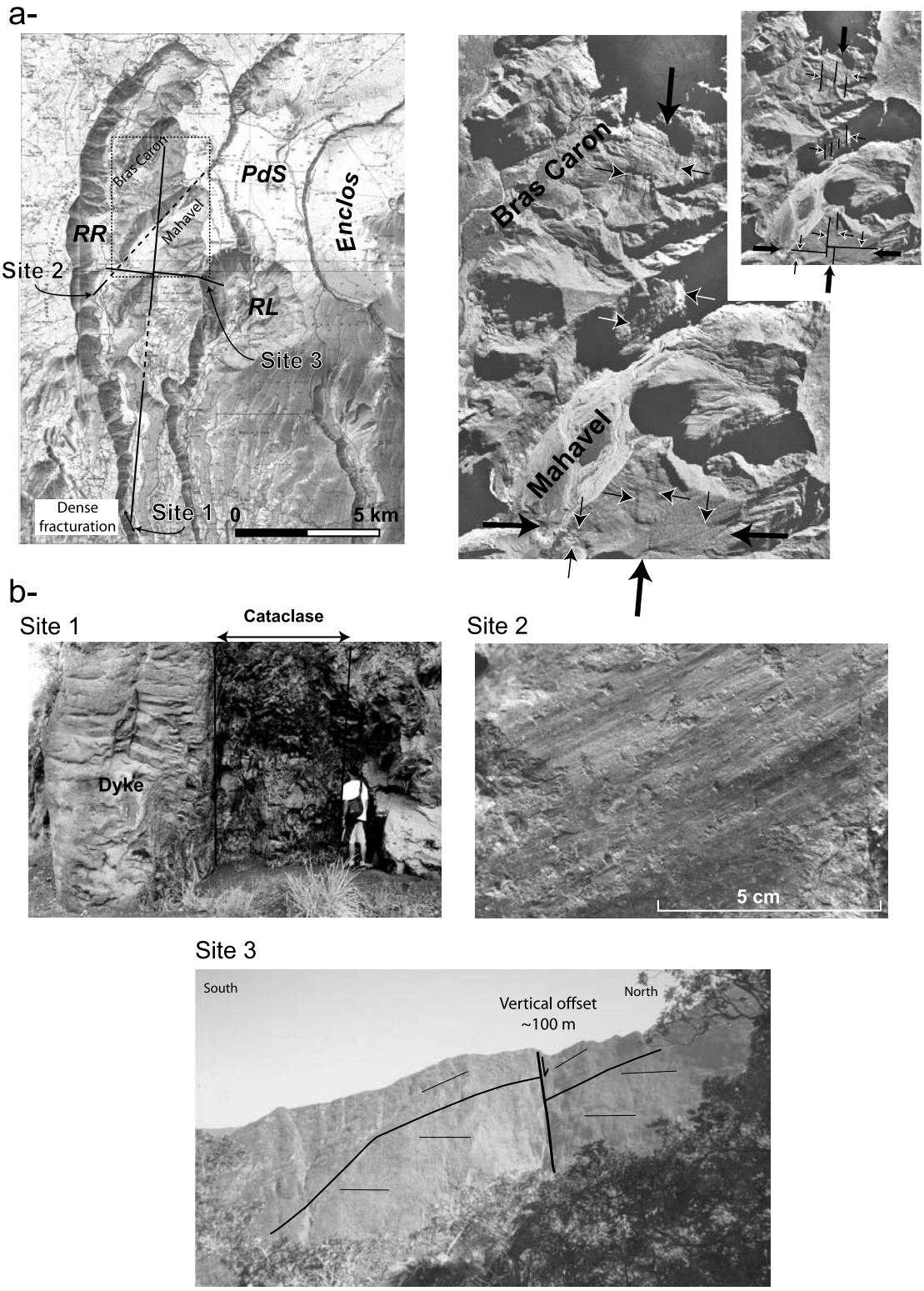

Figure 7

ence could indicate that the structural control of the Alizés volcano is predominant in the eastern half of PdF.

4. Island and Crustal Orientations

4.1. Island Structures

[24] La Réunion Island presents a N120–130 trending elongated shape which corresponds to the alignment of the Piton de la Fournaise, the Plaine des Cafres volcanic zone, and the Piton des Neiges (Figure 10a). In the past decades several structural analyses and geophysical studies were carried out to determine the first order structures of La Réunion Island [e.g., *Malengreau et al.*, 1999; *Lénat et al.*, 2001]. Gravimetric data show two main orientations (N40 and N120–130), which correspond to the orientations of deep gravity anomalies located below PdN and the PdN-PdF alignment, respectively [*Malengreau et al.*, 1999]. Two additional large and old structures (i.e., prior to the formation of PdF) were determined on the island's submarine flanks from a sea-level magnetic survey: a N35 reverse anomaly that corresponds to the continuity of a rift zone of PdN, and a N80 reverse anomaly east of PdF which is interpreted as a remnant of the Alizés volcano (Figure 10b) [*Lénat et al.*, 2001].

[25] Geological and structural analyses carried out in the three central depressions of PdN (i.e., Salazie, Mafate, and Cilaos) and on its outcropping flanks reveal the complexity of PdN and the difficulties to study it. An initial work suggested a polyphase evolution, the development of four paleorift zones presenting a star-like distribution (N10, N45, N120, and N160; Figure 10a) and the formation of three main fault trends (N30, N70, and N120) [*Chevallier*, 1979]. Additional studies confirmed the occurrence of radial intrusion and fracture trends with slight differences of 5–10° in orientation which corresponds to the expected error related to the measure of old structures in scarps [*Robert*, 1980; *Haurie*, 1987; *Rocher*, 1988]. If the recent investigations confirm the fracture orientations, observations in the central depressions combined with geophysical data partly disagree with the rift zone distribution as it was initially proposed. For instance, in the Cilaos depression where a N10 rift zone should have existed in the eastern part of the depression [*Chevallier*, 1979], *Maillot* [1999] highlighted two main N30 and N55 intrusion trends in the western margin of the depression and did not observe any N10 trending dyke. It is important to note that most of the geological formations outcropping in the depressions correspond to debris avalanche deposits [*Bret et al.*, 2003; *Oehler*, 2005; *Arnaud*, 2005]. It is likely that a significant part of the dykes measured in previous studies consists of displaced intrusions. Moreover, the only well-developed rift zone in the S flank, the N35 Etang Salé rift zone, which presents cone alignment, a topographic ridge in bathymetry and a strong magnetic anomaly, was not considered previously (Figure 10a). This rift zone is connected to the summit of PdN by the N30 intrusions which turn to N55 close to the summit. Hence the occurrence of the N10 rift zone in the southern part of Piton des Neiges is highly questionable. It is hard to evaluate with the available data the other rift zones (i.e., N45, N120, and N160). Nevertheless, the N40 orientation of the apex of the gravimetric anomaly of PdN suggests a magmatic system which could explain the development of the N45 rift zone on the NE flank of PdN. It subsequently follows a ~N40 structural alignment between the N35 Etang Salé rift zone and the N45 rift zone on the SW and NE flanks of PdN, respectively. The dykes related to the N120 rift zone are mainly observed in the western part of La Montagne Massif, the Mafate depression and east of PdN. This intrusion direction also corresponds to (1) the overall orientation of the Plaine des Cafres volcanic zone which was interpreted as controlled by crustal structures [e.g., *Chevallier*, 1979; *Michel and Zlotnicki*, 1998] and (2) the gravimetric anomaly which links the PdF and PdN [*Malengreau et al.*, 1999]. The N120 orientation is consequently a strong structural orientation that influenced the dyke intrusion. Finally, the N160 rift zone was determined in the eastern part of La Montagne massif and in the Rivière Saint-Denis where a dense dyke network outcrops (Figure 3). Contrary to the N35, N45, and N120 rift zones, the N160 rift zone is not correlated with gravimetric or magnetic data. This could suggest that this intrusion path is of minor importance or is structurally shallower than the three other rift zones. In summary, three main rift zones are recognized at PdN: the N35 rift zone on the S flank, the N45 rift zone on the NE flank, and the N120 which affects both the WNW and ESE flanks.

[26] Different bathymetric campaigns revealed the presence of huge amount of mass deposits on the submarine flanks of La Réunion Island [*Lénat et al.*, 1990; *Labazuy*, 1996; *Bachèlery et al.*, 2003; *Oehler et al.*, 2004]. The Digital Terrain Model shows that the debris avalanche deposits are incised by deep channels which are connected to active or ancient rivers (Figure 11a). Additional erosion structures are interpreted as secondary submarine slides [*Oehler*, 2005]. The lack of geophysical data and the precision of the DTM which strongly varies around the island make a determination of active faults very hard. Nevertheless, one can note that some of the deep channels that incise the debris avalanche deposits or some straight escarpments are locally strikingly linear and oblique to the slope. We propose that the alignment of the subaerial fault zones inferred in the present study with straight lineaments on the submarine flank indicates a fault origin of part of the lineaments visible on the DTM. To this respect, the N05

Figure 7. (a) Location of the three main fault zones visible in the Rivière des Remparts and Rivière Langevin. The black lines do not correspond to the exact fault trace but to the overall fault zone location. Aerial photographs showing the trace of the N05 and N95 faults. The small arrows highlight the visible traces in the valley flanks. (b) At site 1 the N05 fault induced a brecciation of the lava flows of the ''ancient'' Fournaise and was subsequently followed by a basaltic dyke of the present-day Fournaise. At site 2 outcrops the N40 strike-slip fault, which is aligned with the Bras de Mahavel, suggesting that the valley formation was probably controlled by the fault orientation. Site 3 allows determination of a 100 m offset caused by the N95 fault. Note the angular unconformity between the planar lava flows located in the lower part of the rampart and the upper lava flows, which filled the paleovalley 60 ky ago (photo: Jean-Lambert Join).

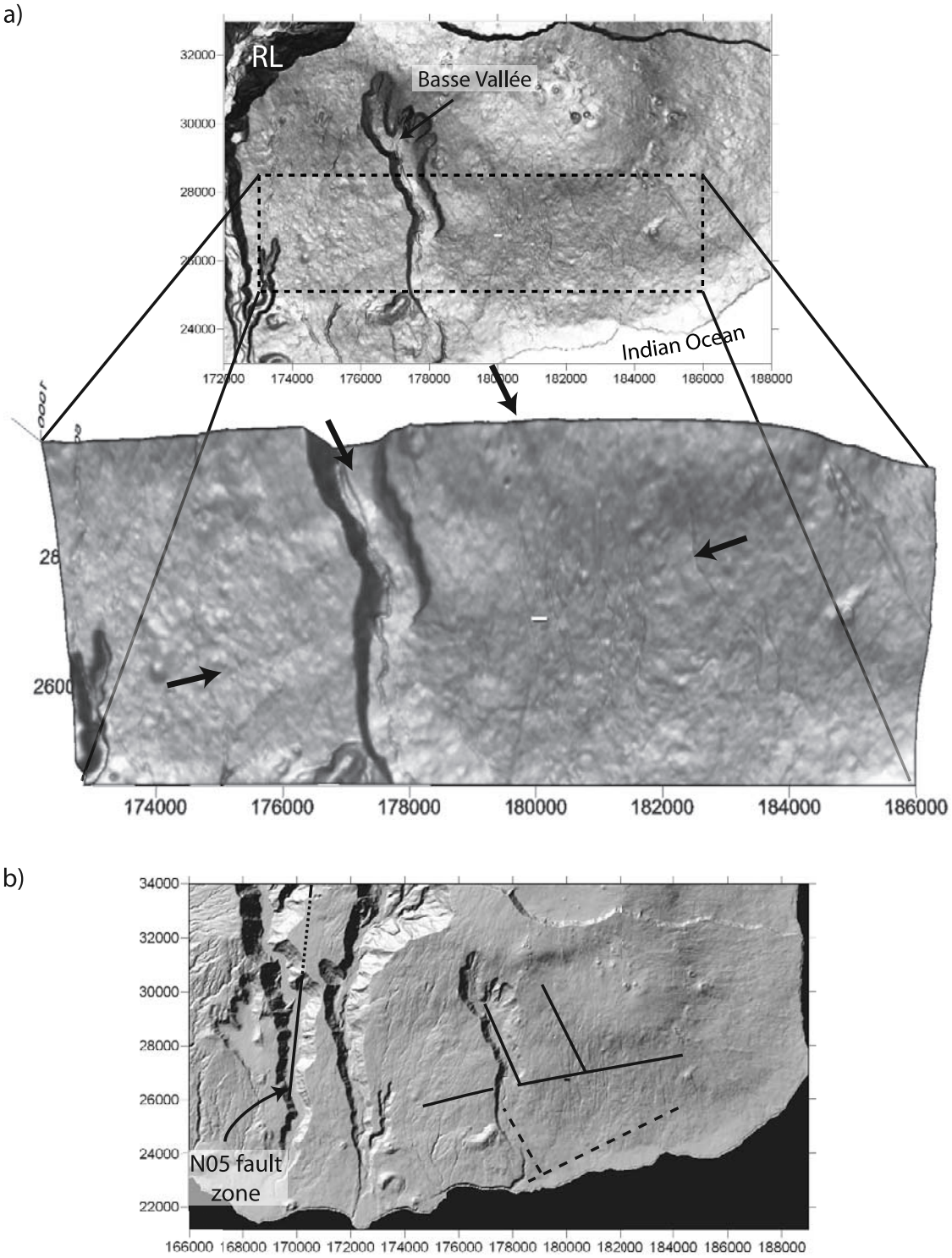

Figure 8. (a) Greyscale slope map representation of the southern flank of PdF. Arrows highlight the main lineaments. RL: Rivière Langevin. (b) Distribution of the main tectonic structures that affect the volcano flank. Dotted lines represent the faults inferred from audiomagnetotellurics method [*Courteaud et al.*, 1996]. The N05 fault zone observed in the Rivière des Remparts is added. Coordinates in meters (Gauss Laborde–Réunion).

trending fault zone observed in the Rivière des Remparts is aligned with the N05 lineament visible in the submarine topography (Figure 11a). Considering the length of this lineament and its continuation on the island, a total length of 45–50 km can be inferred for the fault zone. The northern margin of the Eastern Plateau corresponds to a N75 linear scarp, which is aligned with the N70–75 fault zone that affects the PdF northern flank and the N80 reverse magne-

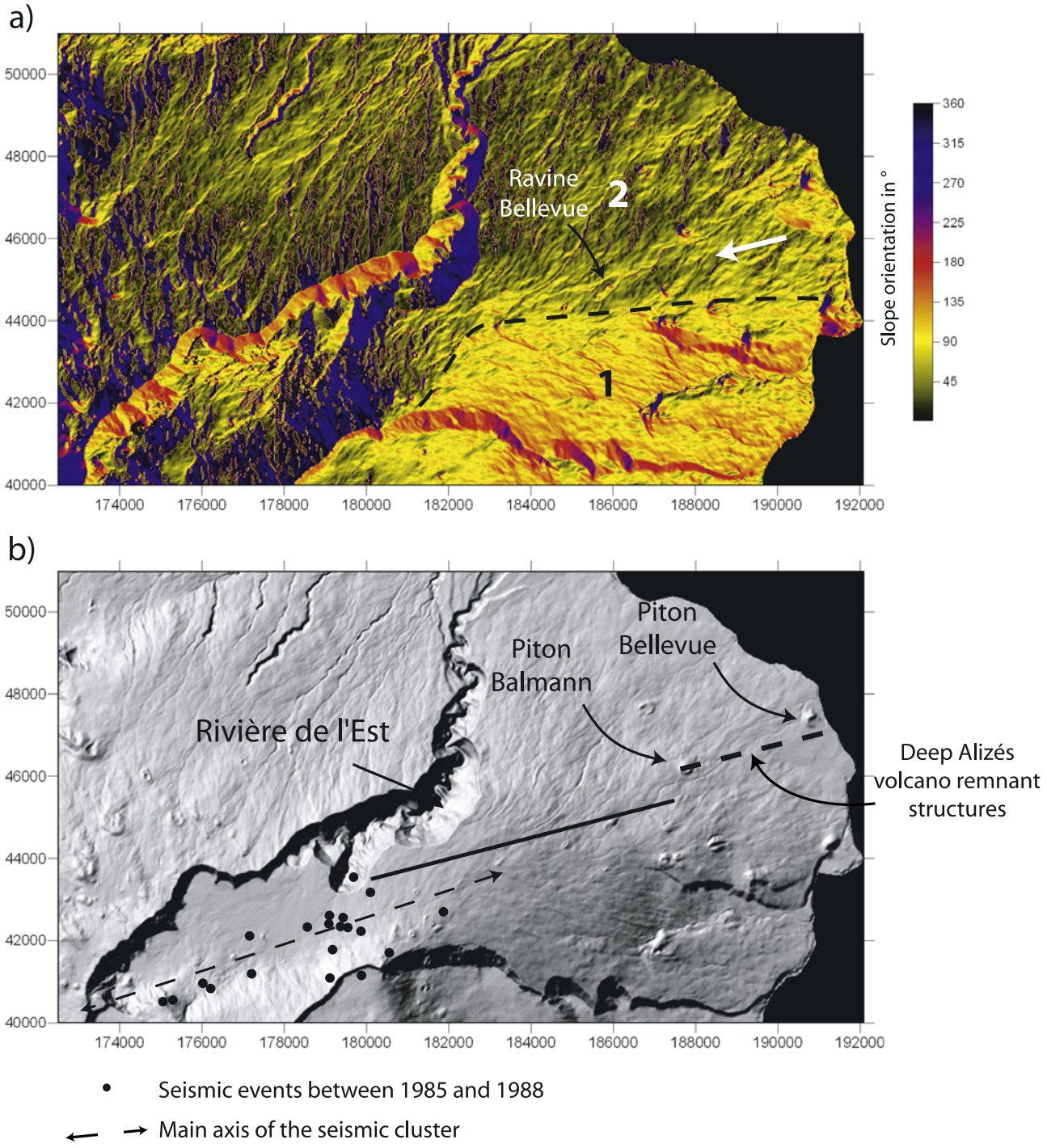

Figure 9. (a) Slope orientation map of the northern flank of PdF. 1 and 2 correspond to two different slope domains. The white arrow highlights the N70–75 trending kilometer-long lineament of the Ravine Bellevue. (b) Shaded relief representation (artificial illumination from the NW) of the northern flank of PdF. The thick dotted line indicates the location of a strong reverse magnetised body [*Michel and Zlotnicki*, 1998]. Black dots represent the earthquakes recorded between 1985 and the end of 1988 [*Nercessian et al.*, 1996]. Note that the earthquakes are distributed along a main N70–75 axis, which is parallel to the Ravine Bellevue lineament and the deep reverse magnetised body. Coordinates in meters (Gauss Laborde–Réunion).

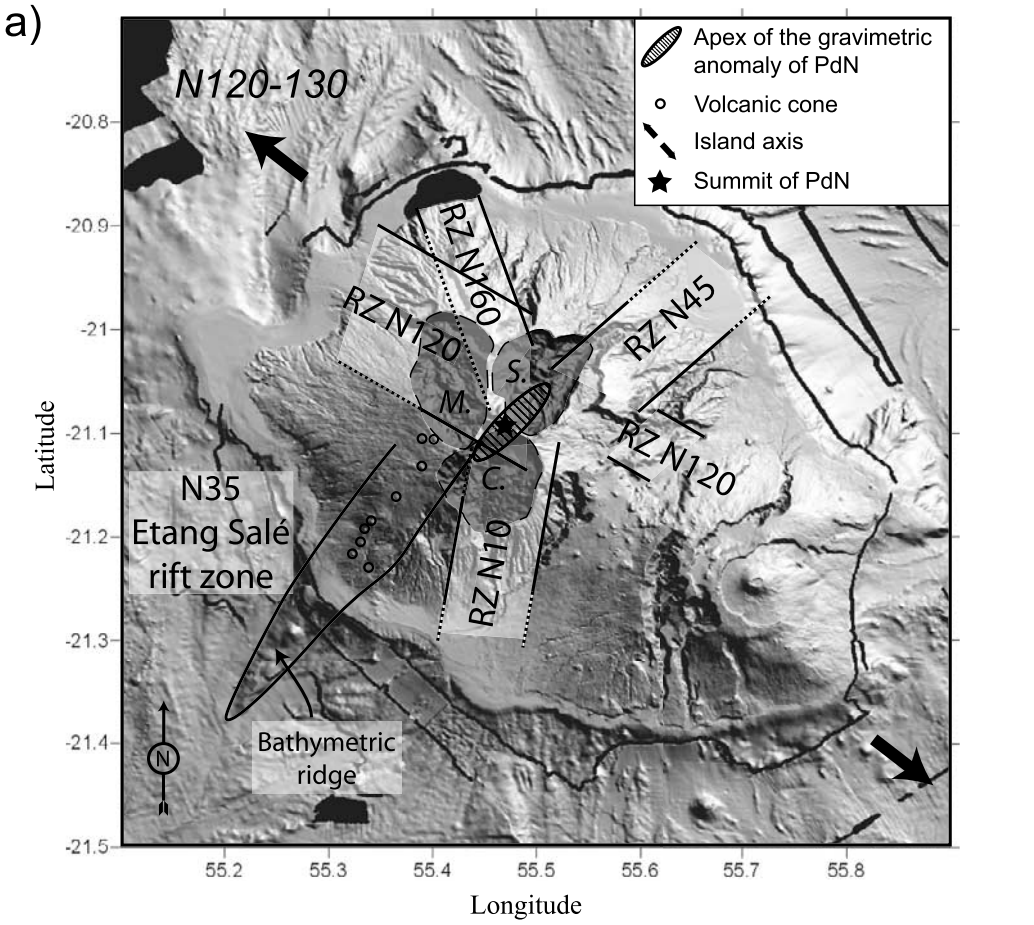
a)
N120-130
Apex of the gravimetric anomaly of PdN
Volcanic cone
Island axis
Summit of PdN
RZ N160
RZ N120
RZ N45
RZ N120
RZ N10
S.
M.
C.
N35
Etang Salé
rift zone
Bathymetric
ridge
N
Latitude
Longitude
-20.8
-20.9
-21
-21.1
-21.2
-21.3
-21.4
-21.5
55.2
55.3
55.4
55.5
55.6
55.7
55.8

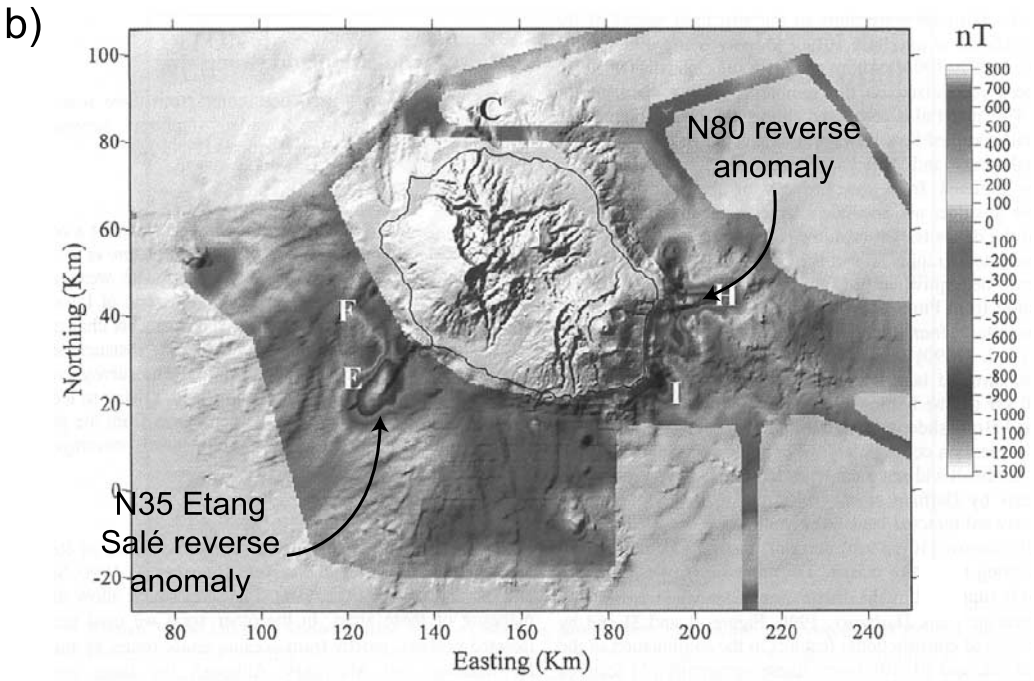
b)
nT
800
700
600
500
400
300
200
100
0
-100
-200
-300
-400
-500
-600
-700
-800
-900
-1000
-1100
-1200
-1300
C
N80 reverse
anomaly
H
F
E
I
N35 Etang
Salé reverse
anomaly
Northing (Km)
Easting (Km)
100
80
60
40
20
0
-20
80
100
120
140
160
180
200
220
240

Figure 10

tized anomaly. Such an alignment between the structures could be explained by the occurrence of a large N70–N80 fault in the eastern part of the edifice. Finally, the southern submarine flank of PdF is characterised by a N150 lineament for which sonar images show that it does not consist of either a geological limit or an incised channel (Figure 11b). It is noteworthy that the N145–150 direction also corresponds to clear lineaments and geophysical structures (inferred from time domain electromagnetic and audiomagnetotelluric methods) in the southern subaerial flank of PdF (Figure 8). Thus we show that the different faults observed in the subaerial part of PdF coincide with those on a larger scale.

4.2. Oceanic Crust Orientations

[27] Recent aeromagnetic, sea level magnetic, seismic surveys, and bathymetric data allowed the determination of the structures of oceanic crust in the surrounding areas of La Réunion and Mauritius Islands [*Dyment*, 1991; *de Voogd et al.*, 1999; *Lénat et al.*, 2001]. Around the islands, the lithosphere shows N30–40 transform zones and N120–130 trending magnetic anomalies (Figure 1a). The N120–130 crustal orientation is also present below the island as suggested by the global alignment of the magmatic massifs of La Réunion, and the elongated seamount located on the western submarine flank (Figure 11a). This general pattern with two main crustal orientations changes between La Réunion Island and the Mauritius transform zone where magnetic anomalies trend in the N80 direction. The presence of this crustal orientation below the eastern part of the volcanic edifice has been revealed by seismic data, which show the occurrence of a N80 trending basement high below the Eastern Plateau [*de Voogd et al.*, 1999]. Bathymetric data [*Smith and Sandwell*, 1997; *Fretzdorff et al.*, 1998] indicate that south of the island the crust is characterized by N55–60 trending topographic ridges and elongated seamounts, which continue below the eastern part of the island (Figure 12a).

5. Discussion and Conclusions

5.1. Scale Integration

[28] Our study aimed at the characteristics of tectonic and volcanic structures at different scales allowing comparison of large and small-scale structures (i.e., oceanic crust, submarine and island structures, volcano faults, and eruptive fissures).

[29] We showed that each structural level is characterized by several structural orientations. It is hard to discriminate for a given structural level alone whether the different structures are related to large-scale processes or to local effects due to the intraedifice stress field or volcano evolution. However, the combination of several scales allows distinction of these origins. Indeed, structures induced by local effects such as the intraedifice deformation, the landslide-induced stress field, or magmatic overpressure are restricted to the edifice, whereas large-scale deformation may influence the development of multiscale structures. To this respect, the data show the recurrence of several structural trends from the crustal scale to the small-scale magmatic system of PdF (i.e., N30–40, N70–80, and N120–130; Figure 12b). The N30–40 and N120–130 trends correspond to (1) preferential directions of magmatic intrusion at both PdF and PdN, (2) the elongation of dense intrusive complexes in PdN and between PdF and PdN [*Malengreau et al.*, 1999], (3) two of the main fault trends of PdN [*Chevallier*, 1979], and (4) the regional orientations of the transform zone and spreading center. Even though the N70 faults are observed in PdN [*Chevallier*, 1979], the N70–80 structural direction is mainly restricted to PdF and between PdF and the Mauritius transform zone. This structural orientation is represented by (1) surface and subsurface structures in the N and S flanks of PdF (Figures 8 and 9), (2) a strong reverse anomaly below the E submarine flank (Figure 10b) [*Lénat et al.*, 2001], (3) an elongated basement high [*de Voogd et al.*, 1999], and (4) the local crustal fabrics revealed by magnetic anomalies (Figure 1). We interpret the parallelism between the magmatic, the island scale, and crustal structures as resulting from a structural control played by the oceanic crust in the past and present construction of La Réunion's volcanoes.

[30] Other structures such as the N05 fault zone south of PdF or the N160 rift zone of PdN, which are spatially isolated and not observed at different structural levels may formed as the consequence of independent geological processes. Local geological events such as flank destabilization are able to control the development of volcanic rift zones [e.g., *Tibaldi*, 2003; *Walter and Troll*, 2003]. The deformation of a volcano above a décollement level [e.g., *Merle and Borgia*, 1996] is an additional feature to decouple the structural influence of both the oceanic crust and the volcanic edifice. In consequence, we consider that the secondary structural directions in La Réunion's volcanoes may result from intraedifice processes rather than a regional stress-field.

5.2. Origin of the Large-Scale Deformation

5.2.1. General Context

[31] La Réunion Island is located east of Madagascar and on the southeastern rim of the Mascarene Basin. Magnetic anomalies indicate that this basin results from oceanic extension between the Campanian (Late Cretaceous; anomaly 34) and the Early Paleocene (anomaly 27 [e.g., *Dyment*, 1991]). This extension was accommodated by large transform zones such as the Wilshaw Ridge and the Mauritius Transform Zone (Figure 1a). Between these two transform zones, the age and the structure of the crustal domain on which La Réunion Island is built are poorly constrained.

Figure 10. (a) Digital Terrain Model (DTM) of the sub-aerial part and proximal sub-marine flanks of La Réunion Island. The island presents a N125-130 elongation. According to *Chevallier* [1979], the magmatic intrusions of Piton des Neiges were restricted to four rift zones (N10, N45, N120, and N160). Note that the well-developed Etang-Salé rift zone, which forms a submarine ridge and is characterized by a cone alignment, was not considered by *Chevallier* [1979]. (b) Sea-level magnetic map showing the N35 reverse magnetized anomaly of the Etang-Salé rift zone. The N80 reverse magnetized anomaly east of the Piton de la Fournaise is interpreted as a remnant part of the Alizés volcano (after *Lénat et al.* [2001]).

Dyment [1991] proposed that the island is located at the intersection of a small-scale transform zone and a paleoridge. Whatever the exact structure, the age of the oceanic spreading in the Mascarene Basin suggests that the transform zones are tectonically inactive since 60 m.y. Consequently, the recent, active deformation determined in the present study and the seismicity on an island scale are

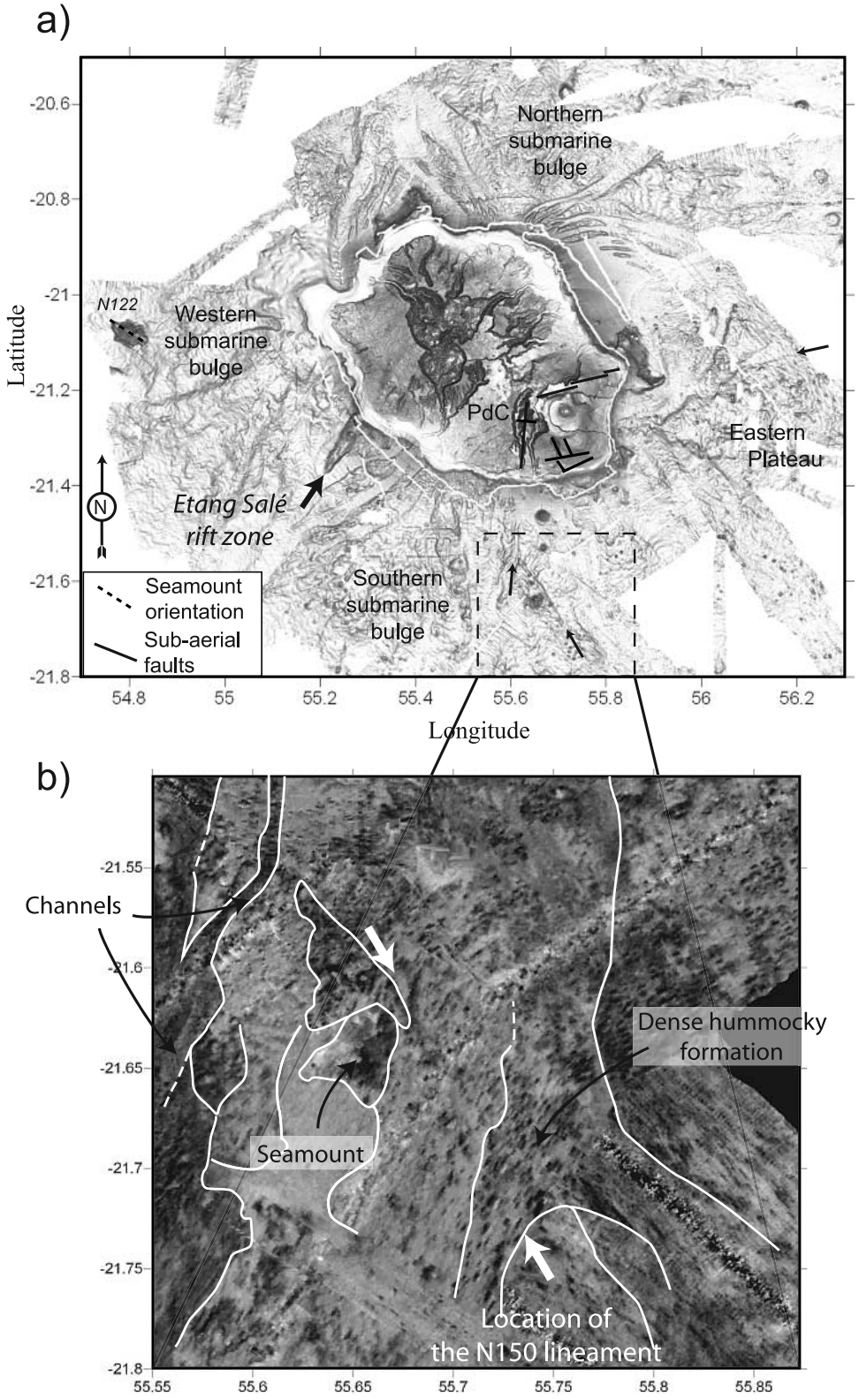

Figure 11

hardly explainable by the present-day activity of the paleoridge and the transform zones.

5.2.2. Effect of the Mantle Plume and the Magmatic Underplating

[32] Geophysical campaigns in the past decades have allowed the determination of the crustal topography around and below the main volcanic islands [*Watts et al.*, 1985; *Binard et al.*, 1991; *Watts et al.*, 1997; *de Voogd et al.*, 1999; *Ali et al.*, 2003]. Large lithospheric flexures have been determined below the Hawaiian chain [*Watts et al.*, 1985] and the Tenerife Island [*Watts et al.*, 1997]. In the island's vicinity, the lithospheric flexure led to the formation of large angular unconformities between prevolcanic and syn/post-volcanic formations [e.g., *Watts et al.*, 1997, Figure 2]. In the Cape Verde Islands, angular unconformities reveal a past crustal flexure during the Miocene, which has been subsequently balanced by a general uplift [*Ali et al.*, 2003]. In contrast to these evolutions, reflection seismic data in La Réunion Island show a lack of angular unconformity, firmly establishing the lack of significant vertical downward movement and flexure [*de Voogd et al.*, 1999]. Furthermore, the base of the edifice that is the top of the preexisting oceanic plate is roughly domed and is characterised by several N55–60 and N80 topographic highs and lows.

[33] The amount of lithospheric flexure is controlled by three main parameters: (1) the size of the volcanic edifice (i.e., the surface load), (2) the elastic thickness of the lithosphere (T_e) which depends on the effective flexural rigidity (D_e) [*Burov and Diament*, 1995], and (3) the subsurface upward loads induced by underplated materials and lithospheric thinning [*Watts et al.*, 1980; *Ali et al.*, 2003]. As the height of La Réunion, Cape Verde, Hawaii, and Tenerife islands are of the same order of magnitude, the downward load due to the volcano weight are roughly similar and it cannot explain alone the differences observed in the crust geometry. One could consider that the lack of lithospheric flexure in La Réunion Island could be caused by different T_e values in La Réunion Island, Hawaii, Cape Verde, and Tenerife. However, T_e values of the oceanic lithosphere are nearly similar in La Réunion (28 km [*Bonneville*, 1990]), Cape Verde (29 km [*Ali et al.*, 2003]), Tenerife (26 km [*Watts et al.*, 1997]), and Hawaii (30–35 km [*Wessel and Keating*, 1994]). Even if the T_e values may present uncertainties due to the complexity of determining the effective flexural rigidity for a oceanic lithosphere (A. Gudmundsson, personal communication, 2006), the "normal" value of lithosphere elastic thickness in La Réunion Island cannot explain the lack of flexure and moreover the slight doming of the edifice basement. Two different processes may produce upward forces and subsequent doming: (1) a thermal erosion of the base of the lithosphere caused by the mantle anomaly and (2) magmatic underplating. The amount of thermally eroded lithosphere and the related uplift depend on the time that a lithosphere stays above a hot anomaly. Large isostatic disequilibrium will be favored in slow plate motion settings and almost nonexistent in fast moving plates (Figure 13). It has been proposed that the displacement of La Réunion Island relative to the hot spot, for the time of known volcanic activity (2.1 My [*MacDougall*, 1971]), was less than 40 km [*Charvis et al.*, 1999]. In such a context, an efficient lithospheric thinning was possible. Furthermore, geophysical data reveal that a large amount of underplated material exists below the southwestern part of La Réunion edifice [*Charvis et al.*, 1999], supporting the underplating hypothesis as an additional cause of the doming.

[34] Hence we interpret the slight crustal doming below La Réunion Island as resulting from a combination of lithospheric thinning due to thermal erosion and magmatic underplating.

5.3. Consequences in the Evolution of La Réunion Volcanoes

[35] The development of a dome-like geometry of the oceanic basement and the occurrence of 500 to 1500 m of pelagic sediments [*de Voogd et al.*, 1999] below the volcanic edifice potentially had strong influences in the evolution of the volcanoes on La Reunion.

[36] The dome-like geometry suggests that the oceanic crust underwent an uplift during the development of the edifice. In a continental setting, the uplift of the lithosphere induces the reactivation of preexisting crustal structures (inherited faults and/or metamorphic fabrics) which subsequently control the location of the volcanism and the geometry of the extension structures [e.g., *Le Gall et al.*, 2004]. In a similar way, we interpret the uplift of the oceanic lithosphere at La Réunion as the motor of the reactivation of the preexisting crustal faults. Such a reactivation can explain the parallelism between the crustal structures and most of the structures observed on the volcanoes. It is obviously wrong to consider that each fault or rift zone observed at the surface is directly linked to reactivated crustal faults. Several additional factors potentially triggered the development of tectonic and magmatic structures. The huge amount of mass deposits on the submarine flanks of the edifice [e.g., *Labazuy*, 1996; *Oehler et al.*, 2004] and in the subaerial part [*Bachèlery et al.*, 2003; *Bret et al.*, 2003] suggests that large flank destabilizations occurred during the evolution of the volcano. The occurrence of large landslides may have produced a rift zone reorientation [e.g., *Walter and Troll*, 2003] and an isostatic deformation [*Smith and Wessel*, 2000]. The deformation of a volcano above low strength layers [*Borgia*, 1994; *Merle and Borgia*, 1996; *Oehler et al.*, 2005] can also develop independent stress fields that lead to the formation of numerous faults. Although a large-scale spreading could have theoretically occurred at La Réunion Island (presence of potential décollement layer at the base of

Figure 11. (a) DTM of the bathymetry showing the distribution of the mass deposits which are mainly concentrated in four bulges (the western, southern, and northern bulges and the Eastern Plateau [*Oehler et al.*, 2004]). The main faults of PdF inferred in this study are represented by black lines. Small arrows indicate the N80, and N05 lineaments visible in the submarine flanks which are aligned with subaerial structures. The N150 lineament is parallel to the structures observed on the southern flank of PdF. Rectangle in dashed line represents the location of Figure 10b. (b) Sonar image of the southern submarine flank of PdF showing the location of the N150 lineament (white arrows) and the distinct geological formations. Note that the lineament does not correspond to either the limit of geological formations or to an incised channel.

a)

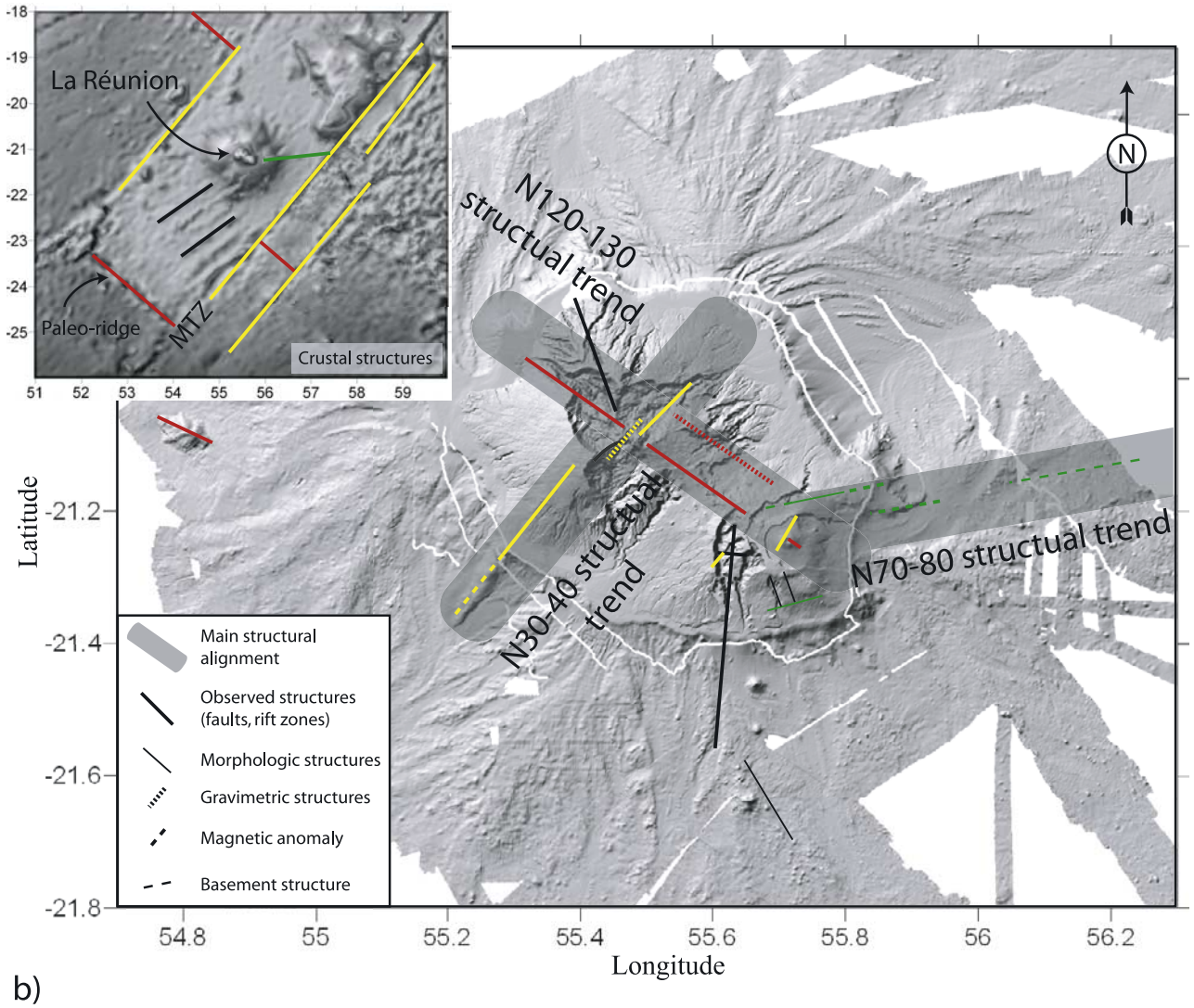

b)

	N30-40 trend	***N55-60 trend***	***N70-80 trend***	***N120-130 trend***
Piton de la Fournaise	N25-30 *(rift zone)*	N55-65 *(structural liniation)*	N75-80 *(structural liniation)*	N125-130 *(rift zone)*
Island structures	N30-40 *(faults, rift zones and intrusive complex at PdN)*		N70-80 *(faults at PdN, crustal highs, remnant of the Alizés volcano)*	N120-130 *(faults, rift zones and intrusive complex at PdN, seamount, island elongation)*
Crustal structures	N30-40 *(transform zones)*	N55-60 *(volcanic ridges)*	N80 *(crustal structure E of La Réunion)*	N120-130 *(regional crustal structure)*

Figure 12. (a) Distribution of the main structures of PdF, PdN, La Réunion edifice and the oceanic crust. Yellow, red and green lines correspond to the N30–40, N120–130, and N70–80 structural trends, respectively. (b) Summary of the main trends observed at different scales: Piton de la Fournaise, island, and crust.

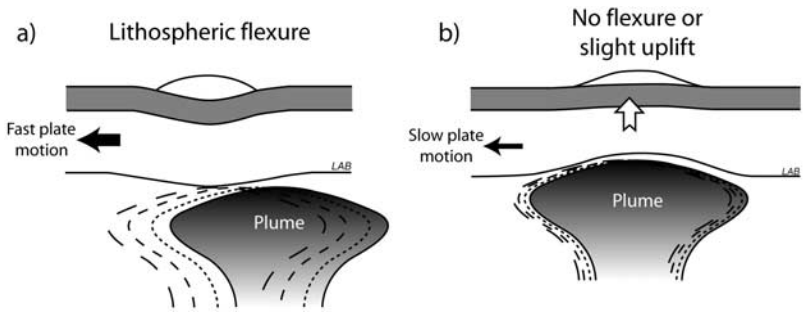

Figure 13. (a) The impact of a plume emplacement below a fast moving plate. The fast plate movement above the mantle anomaly does not allow significant thermal erosion of the base of the lithosphere below the volcanic island. The volcano load subsequently leads to a lithospheric flexure as in Hawaii. Dotted shapes represent the mantle anomaly location at different times. (b) Efficient thermal erosion of a slow moving lithosphere. The thermal erosion induces an isostatic disequilibrium and an uplift of the lithosphere, which at least balances the load of the volcanic edifice. This evolution may partly explain the lack of lithospheric flexure below La Réunion Island.

the edifice), its existence is still unclear. The pelagic sediments below the submarine flanks are undeformed and no expected distal anticline and thrust are observed in reflection seismic data on the SW and NE flank, even several tens of kilometers away from the volcano [*de Voogd et al.*, 1999]. Additional to the large-scale spreading, *Oehler et al.* [2005] proposed that small-scale low strength layers (e.g., deltas and hyaloclastites layers) have induced the edifice deformation and flank landslides.

[37] We therefore propose that the deformation of La Réunion Island and the development of the magmatic rift zones result from the superposition of a general stress field, which is induced by the uplift of the oceanic crust, and local stress fields related to the dynamics and settings of each of the volcanoes.

[38] The volcanoes of La Réunion experienced recurrent flank destabilizations [*Oehler*, 2005]. Recent field observations [*Bachèlery et al.*, 2003; *Bret et al.*, 2003] and analogue experiments [*Merle and Lénat*, 2003; *Oehler et al.*, 2005] suggest that the landslides of La Réunion are due and/or favored by the occurrence of low strength levels in the edifice. Most of these low strength layers correspond to hydrothermally altered materials which mainly develop in the vicinity of the intrusive complex of PdN, PdF, and the Alizés volcano. We propose that the presence of in situ décollement composed of hydrothermally altered and weakened materials is probably not the only cause of a landslide. Indeed, analogue models show that the reactivation in normal faulting mode of crustal preexisting faults below a volcanic edifice leads to the development of normal and reverse faults in the volcano, which can result in gravity instabilities such as flank landslides [*Vidal and Merle*, 2000]. The stability of the edifice decreases when oblique basement faults are simultaneously reactivated and landslides occur after vertical basement displacements of $\sim$150–300 m. Such large amplitudes of vertical displacement are currently not observed in the subaerial part of La Réunion. However, as the faults correspond to the lateral borders of the landslides, the initial offsets related to the reactivation of the basement fault would have not been preserved in the upper part of the edifice. Moreover, the analogue experiment of *Vidal and Merle* [2000] was carried out with brittle materials only. It has been widely demonstrated that the occurrence of low strength materials in volcanoes is a crucial parameter in the deformation and the destabilization of the edifice [e.g., *Siebert*, 1984; *Day*, 1996; *Cecchi et al.*, 2005] We hypothesize that the deformation related to the reactivation of the basement fault would be enhanced by the presence of hydrothermally weakened material in the edifice. Part of the widespread landslides in La Réunion Island would consequently result from the combination of basement fault reactivation and the occurrence of hydrothermally altered materials.

[39] **Acknowledgments.** The authors want to thank Andrea Borgia, Olivier Merle, and Jurgen Neuberg for their constructive comments on the initial version of the manuscript. Philippe Mairine guided us in the Rivière des Remparts. Thanks are also given to Jean-Luc Froger, Philippe Labazuy, and Jean-Francois Lénat for stimulating discussions on the volcano evolution and to Jean-François Oelher who provided the DTM of the bathymetry. Valerie Ferrazzini kindly provided the map of the island seismicity. The reviews of Joan Marti and Agus Gudmundsson helped in the improvement of the manuscript. This work was partly funded by the BQR 2004 provided by the University of La Réunion to L.M.

References

Ali, M. Y., A. B. Watts, and I. Hill (2003), A seismic reflection profile study of lithospheric flexure in the vicinity of the Cape Verde Islands, *J. Geophys. Res.*, *108*(B5), 2239, doi:10.1029/2002JB002155.

Arnaud, N. (2005), Les processus de démantèlement des volcans; le cas d'un volcan bouclier en milieu océanique: Le Piton des Neiges (Ile de la Réunion), Ph.D. thesis, 407 pp., Univ. la Réunion, Saint-Denis Messag, France.

Bachèlery, P. (1981), Le Piton de la Fournaise (Ile de la Réunion): Etude volcanologique, structurale et pétrologique, Ph.D. thesis, Univ. é Clermont-Ferrand II, Clermont-Ferrand, France.

Bachèlery, P., and P. Mairine (1990), Evolution volcano-structurale du Piton de la Fournaise depuis 0,53 Ma, in *Le Volcanisme de la Réunion*, edited by J.-F. Lénat, pp. 213–242, Cent. de Rech. Volcanol., Clermont-Ferrand, France.

Bachèlery, P., L. Chevalier, and J.-F. Gratier (1983), Caractères structuraux des éruptions historiques du Piton de la Fournaise, *C. R. Acad. Sci.*, *296*, 1345–1350.

Bachèlery, P., B. Robineau, M. Courteaud, and C. Savin (2003), Avalanches de débris sur le flanc occidental du volcan-bouclier Piton des Neiges (Réunion), *Bull. Soc. Geol. Fr.*, *174*, 125–140.

Battaglia, J., and P. Bachèlery (2003), Dynamic dyke propagation deduced from tilt variations preceding the March 9, 1998, eruption of Piton de la Fournaise volcano, *J. Volcanol. Geotherm. Res.*, *120*, 289–310.

Binard, N., R. Hékinian, J. L. Cheminée, R. C. Searle, and P. Stoffers (1991), Morphological and structural studies of the Society and

Austral hotspot regions in the South Pacific, *Tectonophysics*, *186*, 293–312.
Bonneville, A. (1990), Structure de la lithosphere, in *Le Volcanisme de la Réunion*, edited by J-.F. Lénat, pp. 1–18., Cent. de Rech. Volcanol., Clermont-Ferrand, France.
Borgia, A. (1994), Dynamic basis of volcanic spreading, *J. Geophys. Res.*, *99*, 17,791–17,804.
Bret, L., Y. Fèvre, J.-L. Join, B. Robineau, and P. Bachèlery (2003), Deposits related to degradation processes on Piton des Neiges volcano (Réunion Island): Overview and geological hazard, *J. Volcanol. Geotherm. Res.*, *123*, 25–41.
Burov, E. B., and M. Diament (1995), The effective elastic thickness (T_e) of continental lithosphere: What does it really mean?, *J. Geophys. Res.*, *100*, 3905–3927.
Cayol, V., and F. H. Cornet (1998), Three-dimensional modeling of the 1983–1984 eruption at Piton de la Fournaise volcano, Réunion Island, *J. Geophys. Res.*, *103*, 18,025–18,037.
Cecchi, E., B. van Wyk de Vries, and J. M. Lavest (2005), Flank spreading and collapse of weak-cored volcanoes, *Bull. Volcanol.*, *67*, 72–91.
Chadwick, W. W., Jr., and J. H. Dieterich (1995), Mechanical modeling of circumferential and radial dike intrusion on Galapagos volcanoes, *J. Volcanol. Geotherm. Res.*, *66*, 37–52.
Charvis, P., A. Laesanpura, J. Gallart, A. Hirn, J.-C. Lépine, B. de Voogd, T. A. Minshull, Y. Hello, and B. Pontoise (1999), Spatial distribution of hotspot material added to the lithosphere under la Réunion, from wide-angle seismic data, *J. Geophys. Res.*, *104*, 2875–2893.
Chevallier, L. (1979), Structures et évolution du volcan Piton des Neiges, île de la Réunion: Leurs relations avec les structures du Bassin des Mascareignes, Océan Indien occidental, 187 pp., Ph.D. thesis, Grenoble Univ., Grenoble, France.
Courteaud, M. (1996), Etude des structures géologiques et hydrogéologiques du Massif de la Fournaise par la méthode audiomagnétotellurique, Ph.D. thesis, 212 pp., Univ. la Réunion, Saint-Denis Messag, France.
Courteaud, M., M. Ritz, M. Descloitres, B. Robineau, and J. Coudray (1996), Cartographie AMT du biseau salé sur le flanc sud du Piton de la Fournaise (Ile de la Réunion), *C. R. Acad. Sci.*, *322*, 93–100.
Courtillot, V., D. Besse, D. Vandamme, R. Montigny, J. J. Jaegger, and H. Capetta (1986), Deccan flood basalts at the Cretaceous/Tertiary boundary?, *Earth Planet. Sci. Lett.*, *80*, 361–374.
Day, S. (1996), Hydrothermal pore fluid pressure and the stability of porous, permeable volcano, in *Volcano Instability on the Earth and Other Planets*, edited by W. J. McGuire, A. P. Jones, and J. Neuberg, *Geol. Soc. Spec. Publ.*, *110*, 77–93.
Deniel, C., G. Kieffer, and J. Lecointre (1992), New ^{230}Th and ^{238}U and ^{14}C age determinations from Piton des Neiges volcano, Reunion: A revised chronology for the differenciated series, *J. Volcanol. Geotherm. Res.*, *51*, 253–267.
de Voogd, B., S. Pou Palomé, A. Hirn, P. Charvis, J. Gallart, D. Rousset, J. Dañobeitia, and H. Perroud (1999), Vertical movements and material transport during hotspot activity: Seismic reflection profiling offshore la Réunion, *J. Geophys. Res.*, *104*, 2855–2874.
Duffield, W. A., L. Stieltjes, and J. Varet (1982), Huge landslide blocks in the growth of Piton de la Fournaise, la Réunion, and Kilauea volcano, Hawaii, *J. Volcanol. Geotherm. Res.*, *12*, 147–160.
Dyment, J. (1991), Structure et évolution de la lithosphère océanique dans l'océan Indien: Apports des anomalies magnétiques, Ph.D. thesis, 374 pp., Univ. Strasbourg, Strasbourg, France.
Fèvre, Y., F. Saint-Ange, S. Bonnet, A. Crave, and B. Robineau (2004), Role of groundwater flow in oceanic volcanoes evolution: Experimental modelling and application to la Reunion Island, paper presented at IAVCEI General Assembly 2004, Int. Assoc. of Volcanol. and Chem. of the Earth's Inter., Pucon, Chile.
Fretzdorff, S., P. Stoffers, C. W. Devey, and M. Munschy (1998), Structure and morphology of submarine volcanism in the hotspot region around Réunion Island, western Indian Ocean, *Mar. Geol.*, *148*, 39–53.
Fretzdorff, S., M. Paterne, P. Stoffers, and E. Ivanova (2000), Explosive activity of the Reunion Island volcanoes through the past 260,000 years as recorded in deep-sea sediments, *Bull. Volcanol.*, *62*, 266–277.
Froger, J.-L., Y. Fukushima, P. Briole, T. Staudacher, T. Souriot, and N. Villeneuve (2004), The deformation field of the August 2003 eruption at Piton de la Fournaise, Reunion Island, mapped by ASAR interferometry, *Geophys. Res. Lett.*, *31*, L14601, doi:10.1029/2004GL020479.
Fukushima, Y. (2005), Transferts de magma au volcan du Piton de la Fournaise determinés par la modélisation 3D des données d'interferométrie radar entre 1998 et 2000, Ph.D. thesis, 149 pp., Univ. é Clermont-Ferrand II, Clermont-Ferrand, France.
Fukushima, Y., V. Cayol, and P. Durand (2005), Finding realistic dike models from interferometric synthetic aperture radar data: The February 2000 eruption at Piton de la Fournaise, *J. Geophys. Res.*, *110*, B03206, doi:10.1029/2004JB003268.
Gillot, P.-Y., and P. Nativel (1989), Eruptive history of the Piton de la Fournaise volcano, Reunion Island, Indian Ocean, *J. Volcanol. Geotherm. Res.*, *36*, 53–65.
Gillot, P.-Y., P. Nativel, and M. Condomines (1990), Géochronologie du Piton de la Fournaise, in *Le Volcanisme de la Réunion*, edited by J-.F. Lénat, Cent. de Rech. Volcanol., pp. 243–255, Clermont-Ferrand, France.
Gillot, P.-Y., J.-C. Lefèvre, and P. E. Nativel (1994), Model for the structural evolution of the volcanoes of Reunion Island, *Earth Planet. Sci. Lett.*, *122*, 291–302.
Gudmundsson, A. (2002), Emplacement and arrest of dykes in central volcanoes, *J. Volcanol. Geotherm. Res.*, *255*, 279–298.
Gudmundsson, A. (2006), How local stresses control magma-chamber ruptures, dyke injections, and eruptions in composite volcanoes, *Earth Sci. Rev.*, *79*, 1–31, doi:10.1016/j.earscirev.2006.06.006.
Haurie, J.-L. (1987), Géodynamique des cirques de la Réunion: Implications géotechniques et stabilité des versants, Ph.D. thesis, 284 pp., Univ. Grenoble, Grenoble, France.
Labazuy, P. (1996), Recurrent landslides events on the submarine flank of Piton de la Fournaise volcano (Réunion Island), in *Volcano Instability on the Earth and Other Planets*, edited by W. J. McGuire, A. P. Jones, and J. Neuberg, *Geol. Soc. Spec. Publ.*, *110*, 293–305.
Le Gall, B., L. Gernigon, J. Rolet, C. Ebinger, R. Gloaguen, O. Nilsen, H. Dypvik, B. Deffontaines, and A. Mruma (2004), Neogene-Holocene rift propagation in central Tanzania: Morphostructural and aeromagnetic evidence from the Kilombero area, *Geol. Soc. Am. Bull.*, *116*, 490–510.
Lénat, J.-F.. and P. Bachèlery (1990), Structure and dynamics of the central zone of Piton de la Fournaise volcano, in *Le Volcanisme de la Réunion, Monogr. Cent. De Rech. Volcanol.*, edited by J-.F. Lénat, pp. 257–296, Cent. De Rech. Volcanol., Clermont-Ferrand, France.
Lénat, J.-F., P. Bachèlery, A. Bonneville, and A. Hirn (1989), The beginning of the 1985–1987 eruptive cycle at Piton de la Fournaise (la Réunion): New insights in the magmatic and volcano-tectonic systems, *J. Volcanol. Geotherm. Res.*, *36*, 209–232.
Lénat, J-.F., P. Bachèlery, A. Bonneville, A. Galdéano, P. Labazuy, D. Rousset, and P. Vincent (1990), Structure and morphology of the submarine flank of an active basaltic volcano: Piton de la Fournaise (Réunion Island, Indian Ocean), *Oceanol. Acta*, *10*, 211–223.
Lénat, J.-F., B. Gibert-Malengreau, and A. Galdéano (2001), A new model for the evolution of the volcanic island of Réunion (Indian Ocean), *J. Geophys. Res.*, *106*, 8646–8663.
MacDonald, G. A., and A. T. Abbott (1970), *Volcanoes in the Sea: The Geology of Hawaii*, 441 pp., Univ. Press of Hawaii, Honolulu.
MacDougall, I. (1971), The geochronology and evolution of the young island of Réunion, Indian Ocean, *Geochim. Cosmochim. Acta*, *35*, 261–270.
MacGuire, W. J., and A. D. Pullen (1989), Location and orientation of eruptive fissures and feeder-dykes at Mount Etna: Influence of gravitational and regional tectonic stress regimes, *J. Volcanol. Geotherm. Res.*, *38*, 325–344.
Maillot, E. (1999), Les systèmes intrusifs des volcans boucliers océaniques: Ile de la Réunion (Océan Indien): Approche structurale et experimentale, Ph.D. thesis, 289 pp., Univ. la Réunion, Saint-Denis Messag, France.
Malengreau, B., J.-F. Lénat, and J.-L. Froger (1999), Structure of the Réunion Island (Indian Ocean) inferred from the interpretation of gravity anomalies, *J. Volcanol. Geotherm. Res.*, *88*, 131–146.
Marinoni, L. B., and A. Gudmundsson (2000), Dykes, faults and palaeostresses in the Teno and Anaga massifs of Tenerife (Canary Islands), *J. Volcanol. Geotherm. Res.*, *103*, 83–103.
Merle, O., and A. Borgia (1996), Scaled experiments of volcanic spreading, *J. Geophys. Res.*, *101*, 13,805–13,817.
Merle, O., and J. Lénat (2003), Hybrid collapse mechanism at Piton de la Fournaise volcano, Reunion Island, Indian Ocean, *J. Geophys. Res.*, *108*(B3), 2166, doi:10.1029/2002JB002014.
Michel, S., and J. Zlotnicki (1998), Self-potential and magnetic surveying of la Fournaise volcano (Réunion Island): Correlations with faulting, fluid circulation, and eruption, *J. Geophys. Res.*, *103*, 17,845–17,857.
Morgan, W. J. (1971), Convection plumes in the lower mantle, *Nature*, *230*, 42–43.
Nercessian, A., A. Hirn, J.-C. Lépine, and M. Sapin (1996), Internal structure of the Piton de la Fournaise volcano from seismic wave propagation and earthquake distribution, *J. Volcanol. Geotherm. Res.*, *70*, 123–143.
Oehler, J.-F. (2005), Les déstabilisations de flanc des volcans de l'Ile de la Réunion (Océan Indien): Mise en évidence, implications et origines, Ph.D. thesis, 422 pp., Univ. é Clermont-Ferrand II, Clermont-Ferrand, France.
Oehler, J.-F., P. Labazuy, and J.-F. Lénat (2004), Recurrence of major flank landslides during the last 2 Ma-history of Réunion Island, *Bull. Volcanol.*, *66*, 585–598.

Oehler, J.-F., B. Van Wyk de Vries, and P. Labazuy (2005), Landslides and spreading of oceanic hot-spot and arc shield volcanoes and Low Strength Layers (LSLs): An analogue modelling approach, *J. Volcanol. Geotherm. Res.*, *144*, 169–189.

O'Neill, C., D. Müller, and B. Steinberger (2003), Geodynamic implications of moving Indian Ocean hotspots, *Earth Planet. Sci. Lett.*, *215*, 151–168.

Peltier, A., V. Ferrazzini, T. Staudacher, and P. Bachèlery (2005), Imaging the dynamics of dyke propagation prior the 2000–2003 flank eruptions at Piton de la Fournaise, Réunion Island, *Geophys. Res. Lett.*, *32*, L22302, doi:10.1029/2005GL023720.

Pollard, D. D. (1987), Elementary fracture mechanics applied to the structural interpretation of dykes, in *Mafic Dyke Swarms*, edited by H. C. Halls and W.F. Fahrig, *Geol. Assoc. Can. Spec. Pap.*, *34*, 5–24.

Rançon, J.-P., P. Lerebour, and T. Augé (1989), The Grand Brulé exploration drilling: New data on the deep framework of the Piton de la Fournaise volcano. part 1: Lithostratigraphic units and volcanostructural implicationsm, *J. Volcanol. Geotherm. Res.*, *36*, 113–127.

Robert, D. (1980), Inventaire et analyse systématiques des différents ensembles d'intrusions volcaniques (dykes et sills) de l'île de la Réunion, *Rap. BRGM 80 SGN 532 GTH/80 REU 17,* 71 pp., Bur. de Rech. Geol. et Min., Orléans, France.

Rocher, P. (1988), Contexte volcanique et structural de l'hydrothermalisme recent dans le massif du Piton des Neiges, île de la Réunion: Etude détaillée du cirque de Salazie, Ph.D. thesis, 443 pp., Univ Paris-Sud, Paris.

Siebert, L. (1984), Large volcanic debris avalanches: Characteristics of source areas, deposits, and associated eruptions, *J. Volcanol. Geotherm. Res.*, *22*, 163–197.

Sigmundsson, F., P. Durand, and D. Massonnet (1999), Opening of an eruptive fissure and seaward displacement at Piton de la Fournaise volcano measured by RADARSAT satellite radar interferometry, *Geophys. Res. Lett.*, *26*, 533–536.

Smith, J. R., and P. Wessel (2000), Isostatic consequences of giant landslides on the Hawaiian Ridge, *Pure Appl. Geophys.*, *157*, 114–1097.

Smith, W. H. F., and D. T. Sandwell (1997), Global sea floor topography from satellite altimetry and ship depth soundings, *Science*, *277*, 1956–1963.

Tibaldi, A. (1996), Mutual influence of diking and collapses at Stromboli volcano, Aeolian Arc, Italy, in *Volcano Instability on the Earth and Other Planets*, edited by W. J. McGuire, A. P. Jones, and J. Neuberg, *Geol. Soc. Spec. Publ.*, *110*, 55–63.

Tibaldi, A. (2003), Influence of cone morphology on dykes, Stromboli, Italy, *J. Volcanol. Geotherm. Res.*, *126*, 79–95.

Twidale, C. R. (2004), River patterns and their meaning, *Earth Sci. Rev.*, *67*, 159–218.

van Wyk de Vries, B., and R. Matela (1998), Styles of volcano-induced deformation: Numerical models of substratum flexure, spreading and extrusion, *J. Volcanol. Geotherm. Res.*, *81*, 1–18.

Vidal, N., and O. Merle (2000), Reactivation of basement faults beneath volcanoes: A new model of flank collapse, *J. Volcanol. Geotherm. Res.*, *99*, 9–26.

Walker, G. P. L. (1999), Volcanic rift zones and their intrusion swarms, *J. Volcanol. Geotherm. Res.*, *94*, 21–34.

Walter, T. R., and V. R. Troll (2003), Experiments on rift zone evolution in unstable volcanic edifice, *J. Volcanol. Geotherm. Res.*, *127*, 107–120.

Watts, A. B., J. H. Bodine, and M. S. Steckler (1980), Observations of flexure and the state of stress in the oceanic lithosphere, *J. Geophys. Res.*, *85*, 6369–6376.

Watts, A. B., U. S. ten Brink, P. Buhl, and T. M. Brocher (1985), A multichannel seismic study of lithospheric flexure across the Hawaiian-Emperor seamount chain, *Nature*, *315*, 105–111.

Watts, A. B., C. Pierce, J. Collier, R. Dalwood, J. P. Canales, and T. J. Henstock (1997), A seismic study of lithospheric flexure in the vicinity of Tenerife, Canary Islands, *Earth Planet. Sci. Lett.*, *146*, 431–447.

Wessel, P., and B. Keating (1994), Temporal variations of flexural deformation in Hawaii, *J. Geophys. Res.*, *99*, 2747–2756.

Zlotnicki, J., J.-C. Ruegg, P. Bachèlery, and P. A. Blum (1990), Eruptive mechanism on Piton de la Fournaise volcano associated with the December 4, 1983 and January 18, 1984 eruptions from ground deformation monitoring and photogrammetric surveys, *J. Volcanol. Geotherm. Res.*, *40*, 197–217.

P. Bachelery, L. Michon, and F. Saint-Ange, Laboratoire des Sciences de la Terre de l'Université de la Réunion (LSTUR), Institut de Physique du Globe de Paris, CNRS, UMR 7154, BP7151, 15 rue René Cassin, F-97715 Saint Denis messag 9, France. (laurent.michon@univ-reunion.fr)

T. Staudacher, Observatoire volcanologique du Piton de la Fournaise (OVPF), Institut de Physique du Globe de Paris, CNRS, UMR 7154, F-97418 La Plaine des Cafres, France.

N. Villeneuve, CREGUR, Université de la Réunion, 15 rue René Cassin, F-97715 Saint Denis messag 9, France.